Since January 2020 Elsevier has created a COVID-19 resource centre with free information in English and Mandarin on the novel coronavirus COVID-19. The COVID-19 resource centre is hosted on Elsevier Connect, the company's public news and information website.

Applied Soft Computing 111 (2021) 107696

Contents lists available at ScienceDirect

Applied Soft Computing

journal homepage: www.elsevier.com/locate/asoc

Designing a testing kit supply network for suspected COVID-19 cases under mixed uncertainty approach

Seyyed-Mahdi Hosseini-Motlagh *, Mohammad Reza Ghatreh Samani, Parnian Farokhnejad

School of Industrial Engineering, Iran University of Science and Technology, University Ave, Narmak, 16846, Tehran, Iran

ARTICLE INFO

Article history:
Received 12 March 2021
Received in revised form 3 June 2021
Accepted 2 July 2021
Available online 17 July 2021

Keywords:
COVID-19
Test kits
Specificity
Sensitivity
Multi-stage stochastic programming
$\mathcal{M}e$ measure

ABSTRACT

Motivated by the COVID-19 (C-19) pandemic and the challenges it poses to global health and the medical communities, this research aims to investigate the factors affecting of reduction health inequalities related to the C-19 to tackle the increasing number of outbreaks and their social consequences in such a pandemic. Hence, we design a COVID-19 testing kit supply network (C-19TKSN) to allocate various C-19 test kits to the suspected C-19 cases depending on the time between the emergence of their first symptoms and the time they are tested. In particular, this model aims to minimize the total network cost and decrease false results C-19 test by considering the fundamental characteristics of a diagnostic C-19 test (i.e., specificity and sensitivity). In the sensitivity characteristic, a gamma formula is presented to estimate the error rate of false-negative results. The nature of the C-19TKSN problem is dynamic over time due to difficult predictions and changes in the number of C-19 patients. For this reason, we consider the potential demands relating to different regions of the suspected C-19 cases for various C-19 test kits and the rate of prevalence of C-19 as stochastic parameters. Accordingly, a multi-stage stochastic programming (MSSP) method with a combined scenario tree is proposed to deal with the stochastic data in a dynamic environment. Then, a fuzzy approach is employed based on $\mathcal{M}e$ measure to cope with the epistemic uncertainty of input data. Eventually, the practicality and capability of the proposed model are shown in a real-life case in Iran. The results demonstrate that the performance of the MSSP model is significantly better in comparison with the two-stage stochastic programming (TSSP) model regarding the false results and the total cost of the network.

1. Introduction

1.1. Background and motivational real-case

The latest concern on global health is the ongoing coronavirus outbreak of the infectious disease recently called C-19 disease [1]. The coronavirus has a similar structure to the virus that causes Severe Acute Respiratory Syndrome (SARS) [2]. Like the previous two cases of coronavirus outbreaks in the last two decades (i.e., SARS (2002 and 2003) and Middle East Respiratory Syndrome (MERS) (2012 to present)), the outbreak of C-19 has raised crucial challenges to global health and the medical communities [3]. The lack of production kits for C-19 suspected cases and each kit's error are significant challenges that can cause incorrect diagnosis of infected and disinfected cases. Therefore, due to the increasing number of outbreaks and their social consequences, an appropriate solution should be prepared to mitigate the effects of such outbreaks.

According to the World Health Organization (WHO) report, C-19 tests are essential to control the outbreak and its diagnostic criteria [4]. Diagnostic tests and antibody tests are two test methods to identify C-19. Diagnostic tests are divided into two methods: (I) molecular tests (such as the reverse transcription-polymerase chain reaction (RT-PCR) test) and (II) antigen tests. Detection tests for C-19 disease need different processes and equipment and differ in cost and efficiency. The required kits for molecular tests, diagnostic tests, and antibody tests are *polymerase chain reaction* (PCR), rapid diagnostic test (RDT), and enzyme-linked immunosorbent assay (ELISA), respectively. Generally, the accuracy of PCR kits is significantly greater than the RDT and ELISA tests. However, implementing PCR laboratory testing is more expensive than RDT and ELISA tests. Moreover, the production of PCR kits is limited. However, ELISA kits are more accessible as they have a rapid and easy production process.

Despite the roles of diagnostic tests in controlling C-19 outbreak, the fundamental characteristics of diagnostic tests for C-19 disease (i.e., sensitivity, specificity, and corresponding likelihood

* Corresponding author.
E-mail addresses: motlagh@iust.ac.ir (S.-M. Hosseini-Motlagh), mr_samani@ind.iust.ac.ir (M.R.G. Samani), parnian_farokhnejad@ind.iust.ac.ir (P. Farokhnejad).

https://doi.org/10.1016/j.asoc.2021.107696
1568-4946/

ratios) are mostly unclear [5]. No viral test is 100% reliable as diagnostic specificity and sensitivity pose the risks of false negatives and false positives, respectively. Diagnostic specificity is a test's ability to accurately exclude patients who do not have a specific symptom or disease. Diagnostic sensitivity is a test's ability to better recognize patients with a given illness or disorder [6]. As healthcare systems worldwide are struggling to deal with C-19 disease, concerns have been raised about the constant spread of the disease by people who are infected without symptoms [7,8]. To recognize and solve this problem, some efforts have been undertaken to develop and implement testing protocols and increasing C-19 testing [8]. In this paper, both diagnostic specificity and sensitivity C-19 testing are considered for decreasing the false results.

The uncertain nature of C-19, the severe scarcity of resources for testing and treatment, the safety of responders and health care professionals from infection, growing financial loss of C-19 disease to the healthcare system are the most critical factors which highlight the importance of investigation of supply chain problems related to the C-19 tests [9]. To this end, in this paper, we propose a multi-product C-19TKSN that consists of the regions of suspected C-19 cases, kit manufacturers, fixed testing labs (FTLs), mobile testing labs (MTLs), and specialized hospitals. The C-19TKSN investigates three types of test kits for the regions of the suspected C-19 cases considering the test centers' capacity and production capacity.

Additionally, the nature of the C-19TKSN problem is dynamic over time due to difficult predictions and changes in the number of C-19 patients. The potential demands relating to different regions of the suspected C-19 cases for various C-19 test kits are stochastic. Besides, the rate of prevalence of C-19 is uncertain and quite challenging to be predicted. Accordingly, in this paper, a MSSP method with a combined scenario tree (ST) is proposed to deal with stochastic data in a dynamic environment. Laporte et al. [10] verified that when the uncertainty related to stochastic parameters (SPs) has been progressively realized in each period, the proposed MSSP method is a useful optimization tool.

Furthermore, some of the parameters in this network (e.g., the capacity data for testing centers, opening costs of MTLs, operation costs, transportation costs) are tainted with uncertainty in real-life scenarios due to the dynamic nature of the problem (i.e., possible long-term parameter value fluctuations), which is verified by Mousazadeh et al. [11]. The robustness of the final solution is of significant importance in such a scenario, as it deals with decisions on location–allocation and capacity, which cannot be readily altered in a long-term horizon [12]. Therefore, in this study, a consolidated solution based on a recently developed fuzzy measure is also applied to protect the network against epistemic uncertainty (EU).

1.2. Research questions

To reduce referrals and reduce congestion in test centers, which can lead to a high prevalence of the C-19 disease, MTLs are provided in some areas to improve access for people and reduce the movement and transportation of people among areas and reduce the prevalence of the C-19 disease. According to the issues mentioned above, this study aims to answer the following main questions:

- What policies should be applied for designing a C-19TKSN? What are the optimal number and location of MTLs for the suspected C-19 cases?
- What strategies must be adopted to reduce the risk of false coronavirus test results and the number of incorrect diagnoses under different C-19 testing methods?
- How to cope with uncertainties and mitigate their effects on cost and capacity?
- How should kits be allocated from production companies to testing centers?

In this paper, we design a C-19TKCN to deal with uncertain prognoses, severe scarcity of resources for testing and treatment, and economic and financial losses faced by the healthcare system. This study also aims to reduce false results of C-19 kits by considering proper planning, which incorporates the fundamental characteristics of diagnostic C-19 tests (i.e., specificity and sensitivity). In the sensitivity characteristic, a formula is presented to estimate the error rate of false-negative results, and in the specificity characteristic, we consider the error of the kits as the error rate of false-positive results. Moreover, this study aims to minimize the total network cost and decrease false results through specificity and sensitivity characteristics. Our findings provide meaningful guidance for governments on whether and how to design C-19TKSN during a situation like the C-19 epidemic.

The structure of the paper is as follows. A review of the related literature is provided in Section 2. The problem description and the mathematical formulation are presented in Section 3. In Section 4, solution methodology is presented, including a scenario tree construction procedure, a fuzzy approach based on $\mathcal{M}e$ measure, and a method to solve the multi-objective problem. The case study, computational results, sensitivity analyses, and key findings are provided in Section 5. Finally, the conclusion is presented in Section 6.

2. Literature review

As discussed in the previous section, distributing different C-19 test kits to testing centers, properly allocating kits to reduce disease transmission risk considering limited resources, and correct diagnosis are crucial during the C-19 outbreak. However, in the existing literature, the supply chain network design of C-19 testing kits has paid less attention. This paper focuses on the issues of supply chain network design for C-19 testing kits. To highlight the novelty of this study relative to the prior literature, in this section, two relevant research streams to this study are reviewed: (1) Application of operations research in C-19 outbreak and (2) Application of operations research in health service network design. Finally, research gaps are recognized, and the contributions of this study are discussed.

2.1. Applications of operations research in C-19 outbreak

Some studies have investigated the applications of operational research methods in the C-19 epidemic. For instance, Govindan et al. [13] developed a decision support system to handle demand and alleviate the impact of the C-19 pandemic in the healthcare system. Ivanov [7] proposed a simulation-based method to monitor and predict the possible impacts of the latest pandemic on the supply chain risk of infectious outbreaks. In another study, Ivanov et al. [14] developed interconnected supply networks and durability to ensure survival in the C-19 outbreak using dynamic game theory. Yu et al. [15] proposed a multi-period multi-objective reverse logistics model for managing the medical waste produced during the C-19 outbreak considering the location of temporary facilities and transportation policy to handle the medicinal waste. In another research, Ivanov et al. [16] studied the viability of resiliency, agile, and sustainable operations in supply chains to investigate the long-term effects of the C-19 disease. Choi et al. [17] investigated the impact of the C-19 epidemic on the customers' and service providers' behaviors in the Hong Kong service operating system. Kargar et al. [18] proposed a multi-objective reverse logistics model for infectious medical waste

decisions considering a reliable network using a revised multi-choice goal programming method. Paul et al. [19] developed a recovery model for high-demand and essential items during the C-19 outbreak. Karmaker et al. [20] investigated the drivers of the sustainable supply chain to tackle supply chain disruptions in the C-19 outbreak using a methodology based on the fuzzy theory, total interpretive structural modeling, and Matriced Impacts Cruoses Multiplication Applique a un Casement techniques. Li et al. [21] proposed simulating simple interaction rules of firms inside the supply chain network to examine the disruption propagation.

A review of the literature on the application of operations research in the outbreak of C-19 disease, a substantial proportion of the papers has worked on operations research technics to examine economic and social conditions created by the outbreak of C-19 disease. Operations research techniques can design an efficient treatment network. Additionally, the nature of the C-19TKSN problem is dynamic over time due to difficult predictions and changes in the number of C-19 patients. In order to deal with uncertain situations during outbreaks, decision-makers (DMs) must implement robust and reliable strategies. However, no paper has covered the issue of allocating the C-19 kit test uncertainty by incorporating the fundamental characteristics of C-19 tests (i.e., specificity and sensitivity) to reduce diagnosis risks. To filling the gap, this study is seeking to apply operations research techniques in the design of C-19TKSN.

2.2. Applications of operations research in the health service network design

Several types of research have explored network design for health systems using different operational research methods. Mousazadeh et al. [11] investigated a network design problem for hierarchical three-level health service systems proposing a mixed-integer and a mixed possibilistic robust programming approaches. In another study, Mousazadeh et al. [22] proposed a multi-period three-level health service network, mixed possibilistic-flexible, and augmented ε-constraint approaches to establish a viable, stable, and efficient network for a real-world case. Lucchese et al. [23] developed a location-routing model considering a facility location experimental algorithm, recognition of hub, and location in the healthcare supply chain to minimize warehousing and transportation costs. Beheshtifar and AliMoahmmadi [24] proposed a multi-objective model considering a geographical information system and a multi-objective genetic algorithm to investigate social commitments, costs associated with land acquisition, and incompatibility with land use concerning the establishment of new health facilities in the supply chain network. Shishebori et al. [25] developed a robust optimization method to design a reliable medical service network considering limited budget, system disruptions, and uncertain parameters. Zarrinpoor et al. [26] developed a scenario-based stochastic programming method to develop a two-level reliable hierarchical location–allocation model with service referral. Mohamadi and Yaghoubi. [27] developed a bi-objective stochastic optimization model for determining the location of transfer points and medical supply distribution centers in a triage system network in an urban district in Iran using an ε-constraint method.

In this respect, according to the issues mentioned above, many studies have examined health network design from various aspects. However, no paper has been done for solving the severe scarcity of resources for testing and treatment of C-19 disease. Although Wikramaratna et al. [28] use statistical methods that have estimated the number of negative results of the C-19 test in healthcare, no research focuses on reducing false and positive results using operations research tools. Thus, this paper develops a mathematical model of investigating supply chain problems related to the C-19 tests.

2.3. Contribution statements and research gaps

Due to uncertainties surrounding the extent of the outbreak and the fact that C-19 is a new disease, full information about this disease is not yet available. Additionally, strategies for responding to outbreaks will be influenced by fluctuations in uncertain parameters. Hence, according to what had been studied, DMs should utilize robust and reliable strategies.

When the DM is faced with dynamic structure decisions, time and uncertainty are major factors, it should be able to adopt decision policies that can respond to changes as they unfold. Typically, these decisions correspond with when the DM has access to new information, adjustments, or recourses. The MSSP approach includes models that determine the effects of realized outcomes that were not known prior [29]. The MSSPs are utilized for the supply chain network design in a limited number of papers (please see, e.g., Birge and Louveaux [30], Fattahi et al. [31], Zahiri et al. [32]). In spite of the TSSP approach adopted solely in a single period environment, the MSSP approach was introduced to handle stochastic data during a dynamic (multi-period) environment. The objective of MSSP is to reduce total imposed risk through a scenario tree with its presentation of data uncertainty and its potential impact on the decision sequence [29].

This paper explores the issues raised during the C-19 outbreak considering a real case of Iran to deal with risks, such as errors in the testing result (i.e., false results). To this end, this paper develops a novel integrated C-19TKSN with a multi-stage planning horizon under uncertain demand. According to the literature review on application of operations research in C-19 outbreak and health service network design, the research gap and main contribution of this work are explained as follow:

First, those articles that have considered the application of operations research in the outbreak of C-19 disease, have mostly examined the economic and social consequences created by the outbreak of C-19 disease while no paper has been done for solving the severe scarcity of resources for testing and treatment of C-19 disease. Therefore, the present work proposes an integrated three-echelon multi-period C-19TKSN to production and allocating C-19 test kits to all facilities.

Second, as mentioned, the nature of the C-19TKSN problem is dynamic over time due to difficult predictions and changes in the number of C-19 patients. Therefore, robust and reliable strategies must be implemented to deal with uncertain situations during outbreaks. The proposed MSSP method is a useful optimization tool for uncertainty related to SPs. Hence, we are used MSSP and scenario generation methods via a Monte Carlo simulation approach and a forward scenario reduction technique to convert the scenario fan into a scenario tree.

Third, the present work presents an extended fuzzy method based on the $\mathcal{M}e$ measure that is more flexible and appropriate for making decisions in a fuzzy environment, which is used in order to protect the considered system from uncertainty.

Fourth, as healthcare systems worldwide are struggling to deal with C-19 disease, concerns have been raised about the constant spread of the disease by people who are infected without symptoms. Hence, to solve this problem, we have determined the optimal strategy to select the appropriate kits based on the time of symptoms of people onset incorporating the fundamental characteristics of C-19 tests (i.e., specificity and sensitivity) to reduce diagnosis risks.

The major contributions of this paper can be summarized as follows:

- Designing an integrated three-echelon multi-period supply chain network for C-19 testing;
- Incorporating the fundamental characteristics of C-19 tests (i.e., specificity and sensitivity) to reduce diagnosis risks;

- Determining the optimal strategy to select the appropriate kits based on the time of symptoms of people onset;
- Using MSSP and scenario generation methods via a Monte Carlo simulation approach and a forward scenario reduction technique to convert the scenario fan into a scenario tree;
- Employing a fuzzy approach based on $\mathcal{Me}$ measure to cope with epistemic uncertainty of input data;
- Using a real case study of Tehran city in Iran to demonstrate the suggested model and solution's applicability.

3. Problem definition and mathematical formulation

In this paper, the considered C-19TKSN consists of suspected C-19 cases, kit manufacturers' centers, FTLs, MTLs, and specialized hospitals. As mentioned earlier, three methods are available for testing C-19, which vary in cost and efficiency. Due to the high price of PCR testing equipment, the PCR test's required equipment is only provided in specialized hospitals. For this reason, PCR kits that are performed in MTLs and FTLs should be sent to specialized hospitals. As shown in Fig. 1, in this network, C-19 testing kits flow from kit manufacturers to the testing centers (MTLs, FTLs, and specialized hospitals) for testing suspected C-19 cases. In this paper, a location–allocation problem, including integrated strategic and tactical planning for C-19TKSN, is investigated over a planning horizon to locate MTLs for covering more patients and allocate kits and patients to MTLs and specialized hospitals. The capacity of MTLs is less than FTLs; the main difference between MTLs and FTLs is that the location of MTLs could be changed over the planning horizon with extra costs.

In this model, the kits are allocated to the suspected C-19 cases based on the time between the emergence of their first symptoms and the time they are tested so that the test would be with the best result and the lowest cost. We aim to minimize the number of false test results by observing the fundamental characteristics of a diagnostic C-19 test (i.e., specificity and sensitivity). The model also minimizes the total cost, which consists of the transportation cost of MTLs, transportation cost of kits, kits production cost, purchasing cost of MTLs, and operation cost.

We take: (a) planning decisions as to where locate MTLs and calculate the optimal number of MTLs and (b) operational decisions as allocating the suspected C-19 cases to the MTLs, FTLs, and hospitals, determining the number of kits required in each facility and allocating the kits to suspected C-19 cases based on minimizing the risk of allocating kits from kit manufacturers to MTLs, FTLs, and hospitals. In this study, the following assumptions are considered to model the investigated C-19TSCN.

- The C-19TSCN consists of suspected C-19 cases, kit manufacturers, FTLs, MTLs, and specialized hospitals;
- In this study, multiple sources for kit manufacturing are considered;
- As the location of C-19 testing hospitals and FTLs are given, only the locations of MTLs are calculated in this model;
- It is considered that the MTLs send the tested PCR kits to the hospital at the end of the period;
- The production capacity of kits is limited;
- The considered C-19TKSN is a multi-product and multi-period problem;
- The potential demands of suspected C-19 cases' regions and the rate of prevalence of C-19 are stochastic.

3.1. Estimation of the amount of false-negative error

Health care systems around the world are concerned about an outbreak of C-19 among individuals who have not yet shown symptoms. Globally, the majority of effort has been directed at reducing turnaround times and test sensitivity (i.e., false negatives) [33]; Therefore, C-19 tests are known for false-negative results, which are typically discussed. False-negative rates were found to range from 2% to 33% on repeat sample testing [34].

Wikramaratna et al. [28] have found that the probability of getting a positive result from a test decreases over time after the onset of symptoms of C-19 disease. Considering this fact and owing to the limited number of available test kits, we develop an analytical model that can lead us to find the kits that have fewer errors in diagnosing the probability of getting infected for the patients requested for the test on the rth day after their first symptoms. In other words, when a suspected C-19 patient is to be tested on day r, a decision should be made about using the kit that better suits that day and reduces the risk of false results in the test. To this end, first, the probability of getting false results from a test on the rth day after the onset of the first symptoms of the patient's disease is introduced based on the Gamma distribution function applied in the study by Wikramaratna et al. [28] as:

$$f(x, G, U) = x^{G-1}\frac{\exp(\frac{-x}{U})}{U^{G} * \Gamma(G)} \qquad \forall x > 0 \text{ and } U, G > 0 \tag{1}$$

Using this function, Wikramaratna et al. [28] have estimated the total false-negative rate of results for the hypothetical groups of patients tested. More precisely, they have used a Gamma distribution with parameters of mode ($\mathcal{M}$) and standard deviation ($\boldsymbol{\sigma}$) in which $\mathcal{M}$ shows the highest number of patients who have requested for the test in the rth day after the onset of their first symptoms. The shape parameter (G) and the rate parameter (U) of the gamma distribution are functions of mode ($\mathcal{M}$) and standard deviation ($\boldsymbol{\sigma}$) as in Eqs. (2) and (3):

$$U = (\mathcal{M} + \sqrt{\mathcal{M} + 4\sigma^2})/(2\sigma^2) \tag{2}$$

$$G = 1 + \mathcal{M}U \tag{3}$$

To this end, according to the concept of the probability density function, Take the integral in the desired interval (for example, the first-day interval 0–1) of the Eq. (1) to get the probability of getting false results from a test on the rth day after the onset of the first symptoms of the patient's disease.

The mode and standard deviation of the distribution differ with the time of appearance of the symptoms and the kits used for testing. Specialists need to use various laboratory tests to make a correct diagnosis for separating the infected cases from the uninfected ones. Various tests are available for this purpose, and it is obvious that the test with the least risk and the most accuracy is more suitable for this purpose. However, reaching high levels of test accuracy, e.g., 100% accuracy, is not possible in practice; a test, for various diseases and depending on the conditions will have different accuracy levels.

The impact of undetected cases in medical and social settings, as well as the spread of the epidemic among asymptomatic or mildly symptomatic patients, have always prioritized false-negative results. False-positive results have had severe consequences, particularly among healthcare workers.

The result can also be false-positive if contamination occurs during sample collection, such as a swab accidentally touching a contaminated glove, cross-reacting with different viruses, or reagent contamination. These problems are not only theoretical; As of March 2020, the US Centers for Disease Control and Prevention had to withdraw C-19 test kits because reagent contamination heightened the rate of false positives [35].

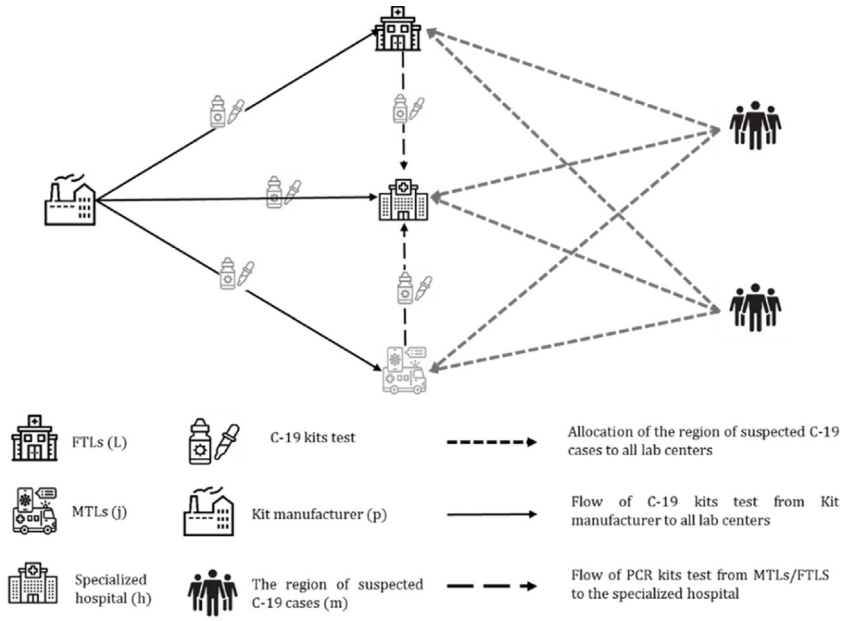

Fig. 1. C-19 testing kits supply chain network.

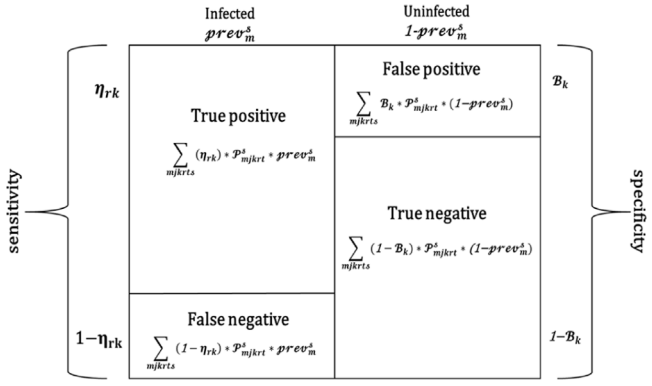

Fig. 2. Schematic representation of coronavirus test analysis.

The fundamental characteristics of diagnostic tests for C-19 disease, which express the above condition, are expressed in sensitivity and specificity; the method is straightforward to be used, but the C-19 disease reacts differently on different days. For this reason, in this paper, to apply the sensitivity and specificity characteristics, we divide the suspected C-19 cases into two groups of infected and uninfected based on the prevalence rate. Accordingly, we calculate the sensitivity characteristics from the Gamma formula, which has been presented to estimate the error rate of the false-negative result, and to calculate the specificity characteristics, we have considered the failure percentage of the submitted kits. η_{rk} and $1-\beta_{\mathrm{k}}$ equal the sensitivity and specificity of the test, respectively. A schematic representation of the coronavirus test analysis network is shown in Fig. 2.

3.2. MSSP formulation

Generally, MSSP with N-stage consists of a series of SPs such as $\Im_1, \Im_2, \ldots, \Im_{N-1}$. A scenario is an explanation of these SPs $\Im_1, \Im_2, \ldots, \Im_{N-1}$ and a ST is used to show random parameters. In fact, a ST is often a set of $\mathcal{S}$ scenarios with the number of scenarios counted by $|\mathcal{S}|$. $p_1, p_2, \ldots, p_{|\mathcal{S}|}$ are the probability of the scenarios and the explanation of SPs for scenario $\mathcal{S} \in \mathcal{S}$ is expressed by $(\Im_1^{\mathcal{S}}, \Im_2^{\mathcal{S}}, \ldots, \Im_{N-1}^{\mathcal{S}})$. Each period is expressed by t ∈ T, hence our model has $|T|$ periods.

In this paper, we consider the suspected C-19 cases' regions demand for various kits and the rate of prevalence of C-19 as SPs, respectively, by $\mathcal{D}_t^{\mathcal{S}}$ and $prev_{mt}^{\mathcal{S}}$ for each scenario $\mathcal{S}$ and period t. Then there is a relation between the stochastic program stages and the planning horizon periods. A typical ST of nine scenarios for four-stage stochastic programming that has three-period planning shows in Fig. 3.

A strategy is non-anticipative in MSSPs that shows the decisions taken at each stage may not depend on the future realization of SPs. There are two common approaches to formulate an MSSP, as shown by Dupacová [36]. At first, a MSSP is formulated as a series of nested TSSPs that the settings for non-anticipativity are indirectly added. The non-anticipativity constraints are explicitly enforced in the second method used in this paper. For more information, refer to Fattahi et al. [31]. $\lambda_n^{\mathcal{S}}$ is the decision vector for stages ∈ {1, 2, …, N}, scenario $\mathcal{S} \in \mathcal{S}$, and decisions must be taken at each stage before SPs are realized. Therefore we have $\lambda_1^{\mathcal{S}} = \lambda_1^{\mathcal{S}'}$ for each pair of scenarios $\mathcal{S}', \mathcal{S} \in \mathcal{S}$ in the first stage of the ST (i.e., in the root node). Besides, for each stage n > 1, we have $\lambda_{n,\mathcal{S}} = \lambda_{n,\mathcal{S}'}$ and scenarios $\mathcal{S}, \mathcal{S}' \in \mathcal{S}$ so that $(\Im_1^{\mathcal{S}}, \Im_2^{\mathcal{S}}, \ldots, \Im_{N-1}^{\mathcal{S}}) = (\Im_1^{\mathcal{S}'}, \Im_2^{\mathcal{S}'}, \ldots, \Im_{N-1}^{\mathcal{S}'})$. If the feasible region for decisions at scenario $\mathcal{S}$ and stage n is $\lambda_{n,\mathcal{S}}$, so we can use the MSSP model (4):

$$Min \sum_{\mathcal{S}=1}^{|\mathcal{S}|} p_{\mathcal{S}} f(\lambda_1^{\mathcal{S}}, \lambda_2^{\mathcal{S}}, \ldots, \lambda_n^{\mathcal{S}} \Im_1^{\mathcal{S}}, \Im_2^{\mathcal{S}}, \ldots, \Im_{N-1}^{\mathcal{S}})$$

Subject to

$$\lambda_n^{\mathcal{S}} \in \lambda_n^{\mathcal{S}'} \quad \forall n \in N \forall \mathcal{S} \in \mathcal{S}$$

$$\lambda_n^{\mathcal{S}} = \lambda_n^{\mathcal{S}'} \quad (\mathcal{S}, \mathcal{S}') \in \mathcal{S}$$

$$\lambda_n^{\mathcal{S}} = \lambda_n^{\mathcal{S}'}$$

$$\forall n \in N/\{1\}, (\mathcal{S}, \mathcal{S}') \in \mathcal{S}: (\Im_1^{\mathcal{S}}, \Im_2^{\mathcal{S}}, \ldots, \Im_{N-1}^{\mathcal{S}}) = (\Im_1^{\mathcal{S}'}, \Im_2^{\mathcal{S}'}, \ldots, \Im_{N-1}^{\mathcal{S}'}) \quad (4)$$

As a conveniently compact form (excluding the second objective function) of the C-19TKSN model could be denoted as

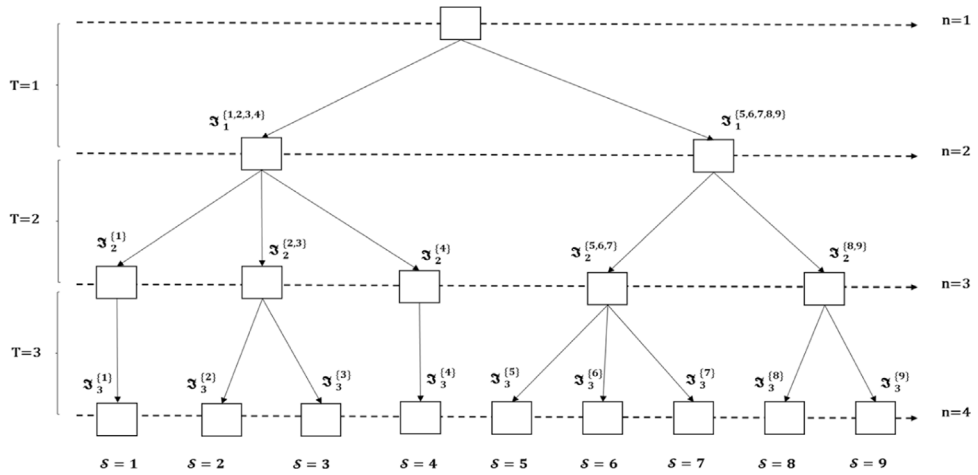

Fig. 3. A scheme of a scenario tree.

follows:

$$\mathcal{M}in\ \mathcal{Z} = \sum_t \mathcal{C}'.\mathcal{Y}_t + \sum_t \mathcal{B}.\mathcal{X}_t$$

Subject to

$$\mathcal{X}_t \le \mathcal{W}.\mathcal{Y}_t \qquad \forall t$$
$$\mathcal{L}.\mathcal{X}_t \ge d_t \qquad \forall t$$
$$\mathcal{V}.\mathcal{X}_t = 0 \qquad \forall t$$
$$\mathcal{H}.\mathcal{Y}_t \le 1 \qquad \forall t$$
$$\mathcal{X}_t \le \mathcal{M}.\mathcal{P}_t \qquad \forall \mathcal{S}, t$$
$$\mathcal{P}_t, \mathcal{Y}_t \in \{0, 1\}, \mathcal{X}_t \ge 0, \tag{5}$$

$\mathcal{C}'$ is equal to the purchasing MTLs cost and $\mathcal{B}$ is equal to Transportation cost, the coefficient matrices of the constraints are the $\mathcal{W}$, $\mathcal{L}$, $\mathcal{V}$, and $\mathcal{H}$ matrices, while $\mathcal{M}$ is a large number. Also, vectors $\mathcal{Y}$ and $\mathcal{P}$ indicate the binary variables, whereas vector $\mathcal{X}$ shows the positive continuous variables. Now assume that vector d representing the demand of the regions of suspected C-19 cases is the stochastic parameter. In the compact formulation, the second objective function is omitted without loss of generality, so it can be acted similarly to the first objective function. According to the above-mentioned, the compact forms of the MSSP models for designing a C-19TKSN formulated as follows:

$$\mathcal{M}in\ \mathcal{Z} = \sum_t \mathcal{C}'.\mathcal{Y}_t + \pi_{\mathcal{S}} \sum_{\mathcal{S}} \mathcal{B}.\mathcal{X}_{t\mathcal{S}}$$

Subject to

$$\sum_{\mathcal{S}} \mathcal{X}_{t\mathcal{S}} \le \mathcal{W}.\mathcal{Y}_t \quad \forall t$$
$$\mathcal{L}.\mathcal{X}_{t\mathcal{S}} \ge d_{t\mathcal{S}} \quad \forall \mathcal{S}, t$$
$$\mathcal{V}.\mathcal{X}_{t\mathcal{S}} = 0 \quad \forall \mathcal{S}, t$$
$$\mathcal{H}.\mathcal{Y}_t \le 1 \quad \forall t$$
$$\mathcal{X}_{t\mathcal{S}} \le \mathcal{M}.\mathcal{P}_{t\mathcal{S}} \quad \forall \mathcal{S}, t$$
$$\mathcal{P}_{t\mathcal{S}} = \mathcal{P}_{t\mathcal{S}'} \quad \forall t = 1(\mathcal{S}, \mathcal{S}') \in \mathcal{S}$$
$$\mathcal{X}_{t\mathcal{S}} = \mathcal{X}_{t\mathcal{S}'} \quad \forall t = 1(\mathcal{S}, \mathcal{S}') \in \mathcal{S}$$
$$\mathcal{P}_{t\mathcal{S}} = \mathcal{P}_{t\mathcal{S}'} \quad \forall t \backslash \{1\}, (\mathcal{S}, \mathcal{S}') \in \mathcal{S} : (\Im_1^{\mathcal{S}}, \Im_2^{\mathcal{S}}, \ldots, \Im_{N-1}^{\mathcal{S}}) = (\Im_1^{\mathcal{S}'}, \Im_2^{\mathcal{S}'}, \ldots, \Im_{N-1}^{\mathcal{S}'})$$
$$\mathcal{X}_{t\mathcal{S}} = \mathcal{X}_{t\mathcal{S}'} \quad \forall t \backslash \{1\}, (\mathcal{S}, \mathcal{S}') \in \mathcal{S} : (\Im_1^{\mathcal{S}}, \Im_2^{\mathcal{S}}, \ldots, \Im_{N-1}^{\mathcal{S}}) = (\Im_1^{\mathcal{S}'}, \Im_2^{\mathcal{S}'}, \ldots, \Im_{N-1}^{\mathcal{S}'})$$
$$\mathcal{P}_{t\mathcal{S}}, \mathcal{Y}_t \in \{0, 1\}, \mathcal{X}_{t\mathcal{S}} \ge 0, \tag{6}$$

As a remark, the compact form of the TSSP model for designing a C-19TKSN is formulated in Appendix A.

3.3. Optimization problem

Here, we give the sets, parameters, and decision variables needed to formulate mathematically the C-19TKSN problem, and then present the mathematical model.

Sets

M	Set of the regions of suspected C-19 cases. ($m \in M$)
J	Set of candidate location of MTLs. $j \in J$, ($j'j'' \in J$).
L	Set of FTLs. ($l \in L$)
H	Set of specialized hospitals. ($h \in H$)
P	Set of kit manufacturers. ($p \in P$)
K	Set of various C-19 test kits. ($k \in K$)
T	Set of periods ($t \in T$, $t = 1, 2, \ldots, \lvert T \rvert$)
R	Set of time between the emergence of their first symptoms and the time they are tested ($r \in R$, $r = 1, 2, \ldots \lvert R \rvert$)
$\mathcal{S}$	Set of scenarios indexed ($\mathcal{S}, \mathcal{S}' \in \mathcal{S}$)

Parameters

$\mathcal{CF}_j$	The purchasing cost of each MTL $j \in J$.
$\mathcal{C}_{j'j''}$	Moving cost of each MTL from location $j' \in J$ to location $j'' \in J$ in two successive periods.
$\mathcal{TRC}'_{pj}$	Transportation cost of all C-19 test kits from kit manufacturer $p \in P$ to MTLs $j \in J$.
$\mathcal{TRC}''_{pl}$	Transportation cost of all C-19 test kits from kit manufacturer $p \in P$ to FTL $l \in L$.
$\mathcal{TRC}'''_{ph}$	Transportation cost of all C-19 test kits from kit manufacturer $p \in P$ to specialized hospital $h \in H$.
$\mathcal{FO}'_{jh}$	Transportation cost of PCR kits from MTL $j \in J$ to specialized hospital $h \in H$.
$\mathcal{FO}''_{lh}$	Transportation cost of PCR kits from FTL $l \in L$ to specialized hospital $h \in H$.
$\mathcal{PC}_k$	Production cost various C-19 test kit $k \in K$
$\mathcal{OC}_j$	Operating cost of MTL $j \in J$.
$\mathcal{OC}'_l$	Operating cost of FTL $l \in L$.
$\mathcal{OC}''_h$	Operating cost of specialized hospital $h \in H$.
η_{rk}	Sensitivity coefficient at the r^{th} day after their first symptoms $r \in R$ for various C-19 kit $k \in K$.

$prev^{\mathfrak{s}}_{mt}$ Rate of the prevalence of C-19 in the regions of suspected C-19 cases $m \in M$ in period $t \in T$ under scenario $\mathfrak{s} \in \mathcal{S}$.
$\mathcal{D}^{\mathfrak{s}}_{mrt}$ Demands of the regions of suspected C-19 cases $m \in M$ at the rth day after their first symptoms $r \in R$ in period $t \in T$ under scenario $\mathfrak{s} \in \mathcal{S}$.
$\mathcal{B}_k$ The failure percentage of C-19 test kit $k \in K$ (specificity coefficient).
$\mathcal{O}_{pkt}$ The maximum production capacity of kit manufacturer $p \in P$ for C-19 test kit $k \in K$ in period $t \in T$.
$ca\mathcal{P}'_{jk}$ The capacity of MTL $j \in J$ for C-19 test kit $k \in K$.
$ca\mathcal{P}''_{lk}$ The capacity of FTL $l \in L$ for C-19 test kit $k \in K$.
$ca\mathcal{P}'''_{hk}$ The capacity of specialized hospital $h \in H$ for C-19 test kits $k \in K$.
μ A very large number.
$\mathcal{P}_{\mathfrak{s}}$ The occurrence probability of scenario $\mathfrak{s} \in \mathcal{S}$.

Positive Variables

$\mathcal{X}'^{\mathfrak{s}}_{mjrt}$ It is equal to 1 if the regions of suspected C-19 cases $m \in M$ is assigned to MTL $j \in J$ on the rth day $r \in R$ in period $t \in T$ under scenario $\mathfrak{s} \in \mathcal{S}$; and 0 otherwise.
$\mathcal{X}''^{\mathfrak{s}}_{mlrt}$ It is equal to 1 if the regions of suspected C-19 cases $m \in M$ is assigned to FTL $l \in L$ on the rth day $r \in R$ in period $t \in T$ under scenario $\mathfrak{s} \in \mathcal{S}$; and 0 otherwise.
$\mathcal{X}'''^{\mathfrak{s}}_{mhrt}$ It is equal to 1 if the regions of suspected C-19 cases $m \in M$ is assigned to hospital $h \in H$ on the rth day $r \in R$ in period $t \in T$ under scenario $\mathfrak{s} \in \mathcal{S}$; and 0 otherwise.
$\mathcal{X}_{j'j''t}$ It is equal to 1 if MTL $j \in J$ moves from location j' in period (t -1) to location j'' in period $t \in T$; and 0 otherwise.
$\mathcal{P}^{\mathfrak{s}}_{mjkrt}$ The number of patients tested from the regions of suspected C-19 cases $m \in M$ in MTL $j \in J$ with test kit $k \in K$ on the rth day after their first symptoms $r \in R$ in period $t \in T$ under scenario $\mathfrak{s} \in \mathcal{S}$.
$\mathcal{P}'^{\mathfrak{s}}_{mlkrt}$ The number of patients tested from the regions of suspected C-19 cases $m \in M$ in FTL $l \in L$ with test kit $k \in K$ on the rth day after their first symptoms $r \in R$ in period $t \in T$ under scenario $\mathfrak{s} \in \mathcal{S}$.
$\mathcal{P}''^{\mathfrak{s}}_{mhkrt}$ The number of patients tested from the regions of suspected C-19 cases $m \in M$ with test kits $k \in K$ on the rth day after their first symptoms $r \in R$ in hospital, $h \in H$ in period $t \in T$ under scenario $\mathfrak{s} \in \mathcal{S}$.
$\mathcal{Y}'^{\mathfrak{s}}_{pjkt}$ The number of C-19 test kit $k \in K$ transported from kit manufacturer $p \in P$ *to* MTL $j \in J$ period, t ∈ T under scenario $\mathfrak{s} \in \mathcal{S}$.
$\mathcal{Y}''^{\mathfrak{s}}_{plkt}$ The number of C-19 test kit $k \in K$ transported from kit manufacturer $p \in P$ to FTL, $l \in L$ in period $t \in T$ under scenario $\mathfrak{s} \in \mathcal{S}$.
$\mathcal{Y}'''^{\mathfrak{s}}_{phkt}$ The number of C-19 test kit $k \in K$ transported from kit manufacturer $p \in P$ to hospital $h \in H$ in period $t \in T$ under scenario $\mathfrak{s} \in \mathcal{S}$.
$\mathcal{F}'^{\mathfrak{s}}_{jht}$ The number of used PCR kits transported from MTL $j \in J$ to hospital $h \in H$ in period $t \in T$ under scenario $\mathfrak{s} \in \mathcal{S}$.
$\mathcal{F}''^{\mathfrak{s}}_{lht}$ The number of PCR kits transported from FTL $l \in L$ to hospital $h \in H$ in period $t \in T$ under scenario $\mathfrak{s} \in \mathcal{S}$.

Integer variable

$\mathcal{N}$ Number of required MTLs.

3.3.1. Objective functions (OF)

The first OF, Eq. (7), minimizes total network cost including the network costs include purchasing cost of MTL, moving costs of each MTLs, the different kits transportation costs from manufacturers to MTLs, FTLs and specialized hospitals, PCR kits transportation costs from MTLs, FTLs to hospitals, production costs of test kits in manufacturers and operating costs in MTLs, FTLs, and specialized hospitals, according to the Possibility of different scenarios. As a remark, detailed calculations regarding all formulations are provided in Appendix B.

Min Z_1 :

$$\sum_{j}\left(\mathcal{CF}_j * \mathcal{N}\right) + \sum_{j'j''t}(\mathcal{X}_{j'j''t} * \mathcal{C}_{j'j''}) + \sum_{pjkt\mathfrak{s}} \mathcal{P}_{\mathfrak{s}} * \mathcal{Y}'^{\mathfrak{s}}_{pjkt} * \mathcal{T}rc'_{pj}$$
$$+ \sum_{plkt\mathfrak{s}} \mathcal{P}_{\mathfrak{s}} * \mathcal{Y}''^{\mathfrak{s}}_{plkt} * \mathcal{T}rc''_{pl}$$
$$+ \sum_{phkt\mathfrak{s}} \mathcal{P}_{\mathfrak{s}} * \mathcal{Y}'''^{\mathfrak{s}}_{phkt} * \mathcal{T}rc'''_{ph} + \sum_{jht\mathfrak{s}} \mathcal{P}_{\mathfrak{s}} * \mathcal{F}'^{\mathfrak{s}}_{jht} * \mathcal{FO}'_{jh}$$
$$+ \sum_{lht\mathfrak{s}} \mathcal{P}_{\mathfrak{s}} * \mathcal{F}''^{\mathfrak{s}}_{lht} * \mathcal{FO}''_{lh} + \sum_{pjtk\mathfrak{s}} \mathcal{P}_{\mathfrak{s}} * \mathcal{PC}_k * \mathcal{Y}'^{\mathfrak{s}}_{pjkt}$$
$$\sum_{pltk\mathfrak{s}} \mathcal{P}_{\mathfrak{s}} * \mathcal{PC}_k * \mathcal{Y}''^{\mathfrak{s}}_{plkt} + \sum_{phtk\mathfrak{s}} \mathcal{P}_{\mathfrak{s}} * \mathcal{PC}_k * \mathcal{Y}'''^{\mathfrak{s}}_{phkt} + ((|T|)$$
$$* (\sum_{J} \mathcal{OC}_j + \sum_{l} \mathcal{OC}'_l + \sum_{h} \mathcal{OC}''_h)) \tag{7}$$

The second OF, Eq. (8), minimizes the risk of testing false results by assigning proper test kits. We divide the suspected C-19 cases into two infected and uninfected groups based on the prevalence rate to apply the sensitivity and specificity characteristics. The first, second, and third terms indicate how false-negative rate results can be reduced. Also, the fourth, fifth, and sixth terms show the reduction of false-positive rate results.

Min Z_2:

$$\sum_{mjkrt\mathfrak{s}} \mathcal{P}_{\mathfrak{s}} * ((1-\eta_{rk}) * \mathcal{P}^{\mathfrak{s}}_{mjkrt} * prev^{\mathfrak{s}}_{mt})$$
$$+ \sum_{mlkrt\mathfrak{s}} \mathcal{P}_{\mathfrak{s}} * ((1-\eta_{rk}) * \mathcal{P}'^{\mathfrak{s}}_{mlkrt} * prev^{\mathfrak{s}}_{mt})$$
$$+ \sum_{mhkrt\mathfrak{s}} \mathcal{P}_{\mathfrak{s}} * ((1-\eta_{rk}) * \mathcal{P}''^{\mathfrak{s}}_{mhkrt} * prev^{\mathfrak{s}}_{mt})$$
$$+ \sum_{mjkrt\mathfrak{s}} \mathcal{P}_{\mathfrak{s}} * (\mathcal{B}_k * \mathcal{P}^{\mathfrak{s}}_{mjkrt} * (1 - prev^{\mathfrak{s}}_{mt}))$$
$$+ \sum_{mlkrt\mathfrak{s}} \mathcal{P}_{\mathfrak{s}} * (\mathcal{B}_k * \mathcal{P}'^{\mathfrak{s}}_{mlkrt} * (1 - prev^{\mathfrak{s}}_{mt}))$$
$$+ \sum_{mhkrt\mathfrak{s}} \mathcal{P}_{\mathfrak{s}} * (\mathcal{B}_k * \mathcal{P}''^{\mathfrak{s}}_{mhkrt} * (1 - prev^{\mathfrak{s}}_{mt})) \tag{8}$$

3.3.2. Constraints

Constraint (9) ensures that the number of suspected C-19 cases go to MTLs, FTLs, and specialized hospitals for taking various C-19 test kits is equal to the total number of the suspected C-19 cases (i.e., infected and uninfected cases).

$$\sum_{jk} \mathcal{P}^{\mathfrak{s}}_{mjkrt} + \sum_{lk} \mathcal{P}'^{\mathfrak{s}}_{mlkrt} + \sum_{hk} \mathcal{P}''^{\mathfrak{s}}_{mhkrt} = \mathcal{D}^{\mathfrak{s}}_{mrt} \quad \forall m, r, t, \mathfrak{s} \tag{9}$$

Constraints (10)–(12) indicate that the total number of various C-19 kits sent to MTLs, FTLs, and specialized hospitals should be greater than the number of suspected C-19 cases tested in MTLs, FTLs, and specialized hospitals, respectively.

$$\sum_{p} \mathcal{Y}'^{\mathfrak{s}}_{pjkt} \geq \sum_{mr} \mathcal{P}^{\mathfrak{s}}_{mjkrt} \quad \forall j, k, t, \mathfrak{s} \tag{10}$$

$$\sum_{p} \mathcal{Y}''^{\mathfrak{d}}_{plkt} \geq \sum_{mr} \mathcal{P}'^{\mathfrak{d}}_{mlkrt} \quad \forall l, k, t, \mathfrak{d} \tag{11}$$

$$\sum_{p} \mathcal{Y}'''^{\mathfrak{d}}_{phkt} \geq \sum_{mr} \mathcal{P}''^{\mathfrak{d}}_{mhkrt} \quad \forall h, k, t, \mathfrak{d} \tag{12}$$

Constraints (13)–(15) ensure that the suspected C-19 cases are allocated respectively to FTLs, MTLs, or specialized hospitals in each period only if the regions of suspected C-19 cases are assigned to MTLs, FTLs, and specialized hospital.

$$\sum_{k} \mathcal{P}^{\mathfrak{d}}_{mjkrt} \leq \mu * \mathcal{X}'^{\mathfrak{d}}_{mjrt} \quad \forall m, j, r, t, \mathfrak{d} \tag{13}$$

$$\sum_{k} \mathcal{P}'^{\mathfrak{d}}_{mlkrt} \leq \mu * \mathcal{X}''^{\mathfrak{d}}_{mlrt} \quad \forall m, l, r, t, \mathfrak{d} \tag{14}$$

$$\sum_{k} \mathcal{P}''^{\mathfrak{d}}_{mhkrt} \leq \mu * \mathcal{X}'''^{\mathfrak{d}}_{mhrt} \quad \forall m, h, r, t, \mathfrak{d} \tag{15}$$

Constraint (16) implies that each region of suspected C-19 cases can be assigned to FTL, MTL, or specialized hospitals. In other words, it is considered that each region of suspected C-19 on the rth day can be allocated to one FTL, MTL, or specialized hospital.

$$\sum_{j} \mathcal{X}'^{\mathfrak{d}}_{mjrt} + \sum_{l} \mathcal{X}''^{\mathfrak{d}}_{mlrt} + \sum_{h} \mathcal{X}'''^{\mathfrak{d}}_{mhrt} \leq 1 \quad \forall m, r, t, \mathfrak{d} \tag{16}$$

Constraint (17) ensures that the number of kits shipped from manufacturers to MTLs, FTLs, and the specialized hospital does not exceed the maximum production capacity. In other words, the number of various kits cannot be more than the maximum production capacity.

$$\sum_{j} \mathcal{Y}'^{\mathfrak{d}}_{pjkt} + \sum_{l} \mathcal{Y}''^{\mathfrak{d}}_{plkt} + \sum_{h} \mathcal{Y}'''^{\mathfrak{d}}_{phkt} \leq \mathcal{O}_{pkt} \quad \forall p, k, t, \mathfrak{d} \tag{17}$$

Constraints (18) and (19) ensure that the number of PCR kits tested in MTLs, FTLs is equal to the used PCR kits sent to the specialized hospital; because of the high cost of PCR testing equipment, the required equipment for the PCR test is only provided in specialized hospitals.

$$\sum_{mr} \mathcal{P}^{\mathfrak{d}}_{mj1rt} = \sum_{h} \mathcal{F}'^{\mathfrak{d}}_{jht} \quad \forall j, t, \mathfrak{d} \tag{18}$$

$$\sum_{mr} \mathcal{P}'^{\mathfrak{d}}_{ml1rt} = \sum_{h} \mathcal{F}''^{\mathfrak{d}}_{lht} \quad \forall l, t, \mathfrak{d} \tag{19}$$

Constraint (20) indicates that the number of various C-19 kits sent to MTLs does not exceed the maximum capacity of MTLs.

$$\sum_{p} \mathcal{Y}'^{\mathfrak{d}}_{pjkt} \leq ca\mathcal{P}'_{jk} \quad \forall j, k, t, \mathfrak{d} \tag{20}$$

Constraint (21) guarantees that the number of various C-19 kits sent to FTLs does not exceed the maximum capacity of FTLs.

$$\sum_{p} \mathcal{Y}''^{\mathfrak{d}}_{plkt} \leq ca\mathcal{P}''_{lk} \quad \forall l, k, t, \mathfrak{d} \tag{21}$$

Constraint (22) indicates that the sum of the number of various C-19 kits sent to specialized hospitals and the number of PCR kits sent to the specialized hospital for testing from MTLs, FTLs does not exceed the maximum capacity of specialized hospitals.

$$\sum_{p} \mathcal{Y}'''^{\mathfrak{d}}_{phkt} + \sum_{j\mathfrak{d}} \mathcal{F}'^{\mathfrak{d}}_{jht} + \sum_{l\mathfrak{d}} \mathcal{F}''^{\mathfrak{d}}_{lht} \leq ca\mathcal{P}'''_{hk} \quad \forall p, h, t, \mathfrak{d} \tag{22}$$

In other words, constraints (20)–(22) indicate that sent various C-19 kits cannot be more than the maximum capacity of MTLs, FTLs, and specialized hospitals.

Constraints (23) and (24) show that only one MTL can be transferred to another candidate region of C-19 suspected cases in each period. Constraint (25) would indicate relocation of MTL in two consecutive periods only if it was in the prior location in the past period. In each period, the number of required MTLs is expressed by constraint (26).

$$\sum_{j'} \mathcal{X}_{j'j''t} \leq 1 \quad \forall j'', t \tag{23}$$

$$\sum_{j''} \mathcal{X}_{j'j''t} \leq 1 \quad \forall j', t \tag{24}$$

$$\sum_{j''} \mathcal{X}_{j'j''t} \leq \sum_{j} \mathcal{X}_{jj't-1} \quad \forall j', t \text{ and } t \geq 2 \tag{25}$$

$$\sum_{j'j''} \mathcal{X}_{j'j''t} = \mathcal{N} \quad \forall t \tag{26}$$

3.3.3. Non-anticipativity constraints

$$\mathcal{X}'^{\mathfrak{d}}_{mjrt} = \mathcal{X}'^{\mathfrak{d}'}_{mjrt} \quad \forall m, j, r, t = 1(\mathfrak{d}, \mathfrak{d}') \in \mathcal{S} \tag{27}$$

$$\mathcal{X}''^{\mathfrak{d}}_{mlrt} = \mathcal{X}''^{\mathfrak{d}'}_{mlrt} \quad \forall m, l, r, t = 1(\mathfrak{d}, \mathfrak{d}') \in \mathcal{S} \tag{28}$$

$$\mathcal{X}'''^{\mathfrak{d}}_{mhrt} = \mathcal{X}'''^{\mathfrak{d}'}_{mhrt} \quad \forall m, h, r, t = 1(\mathfrak{d}, \mathfrak{d}') \in \mathcal{S} \tag{29}$$

$$\mathcal{X}'^{\mathfrak{d}}_{mjrt} = \mathcal{X}'^{\mathfrak{d}'}_{mjrt} \quad \forall m, j, r, t \backslash \{1\}, (\mathfrak{d}, \mathfrak{d}') \in \mathcal{S}: (\mathfrak{I}^{\mathfrak{d}}_1, \mathfrak{I}^{\mathfrak{d}}_2, \ldots, \mathfrak{I}^{\mathfrak{d}}_{N-1}) = (\mathfrak{I}^{\mathfrak{d}'}_1, \mathfrak{I}^{\mathfrak{d}'}_2, \ldots, \mathfrak{I}^{\mathfrak{d}'}_{N-1}) \tag{30}$$

$$\mathcal{X}''^{\mathfrak{d}}_{mlrt} = \mathcal{X}''^{\mathfrak{d}'}_{mlrt} \quad \forall m, l, r, t \backslash \{1\}, (\mathfrak{d}, \mathfrak{d}') \in \mathcal{S}: (\mathfrak{I}^{\mathfrak{d}}_1, \mathfrak{I}^{\mathfrak{d}}_2, \ldots, \mathfrak{I}^{\mathfrak{d}}_{N-1}) = (\mathfrak{I}^{\mathfrak{d}'}_1, \mathfrak{I}^{\mathfrak{d}'}_2, \ldots, \mathfrak{I}^{\mathfrak{d}'}_{N-1}) \tag{31}$$

$$\mathcal{X}'''^{\mathfrak{d}}_{mhrt} = \mathcal{X}'''^{\mathfrak{d}'}_{mhrt} \quad \forall m, h, r, t \backslash \{1\}, (\mathfrak{d}, \mathfrak{d}') \in \mathcal{S}: (\mathfrak{I}^{\mathfrak{d}}_1, \mathfrak{I}^{\mathfrak{d}}_2, \ldots, \mathfrak{I}^{\mathfrak{d}}_{N-1}) = (\mathfrak{I}^{\mathfrak{d}'}_1, \mathfrak{I}^{\mathfrak{d}'}_2, \ldots, \mathfrak{I}^{\mathfrak{d}'}_{N-1}) \tag{32}$$

Constraints (27)–(32) reflect the MSSP's non-anticipation constraints. More descriptions have been given previously on these constraints. The allocation decisions for the regions of suspected C-19 cases ($\mathcal{X}$) must be made before knowing the uncertainty recognition of SPs at each stage of the MSSP. These decisions are $\mathcal{P}^{\mathfrak{d}}_{mjkrt}$, $\mathcal{P}'^{\mathfrak{d}}_{mlkrt}$, $\mathcal{P}''^{\mathfrak{d}}_{mhkrt}$ and Constraints (33)–(35), can be defined as follows:

$$\mathcal{P}^{\mathfrak{d}}_{mjkrt} = \mathcal{P}^{\mathfrak{d}'}_{mjkrt} \quad \forall m, j, r, t, (\mathfrak{d}, \mathfrak{d}') \in \mathcal{S}: (\mathfrak{I}^{\mathfrak{d}}_1, \mathfrak{I}^{\mathfrak{d}}_2, \ldots, \mathfrak{I}^{\mathfrak{d}}_{N-1}) = (\mathfrak{I}^{\mathfrak{d}'}_1, \mathfrak{I}^{\mathfrak{d}'}_2, \ldots, \mathfrak{I}^{\mathfrak{d}'}_{N-1}) \tag{33}$$

$$\mathcal{P}'^{\mathfrak{d}}_{mlkrt} = \mathcal{P}'^{\mathfrak{d}'}_{mlkrt} \quad \forall m, l, r, t, (\mathfrak{d}, \mathfrak{d}') \in \mathcal{S}: (\mathfrak{I}^{\mathfrak{d}}_1, \mathfrak{I}^{\mathfrak{d}}_2, \ldots, \mathfrak{I}^{\mathfrak{d}}_{N-1}) = (\mathfrak{I}^{\mathfrak{d}'}_1, \mathfrak{I}^{\mathfrak{d}'}_2, \ldots, \mathfrak{I}^{\mathfrak{d}'}_{N-1}) \tag{34}$$

$$\mathcal{P}''^{\mathfrak{d}}_{mhkrt} = \mathcal{P}''^{\mathfrak{d}'}_{mhkrt} \quad \forall m, k, r, t, (\mathfrak{d}, \mathfrak{d}') \in \mathcal{S}: (\mathfrak{I}^{\mathfrak{d}}_1, \mathfrak{I}^{\mathfrak{d}}_2, \ldots, \mathfrak{I}^{\mathfrak{d}}_{N-1}) = (\mathfrak{I}^{\mathfrak{d}'}_1, \mathfrak{I}^{\mathfrak{d}'}_2, \ldots, \mathfrak{I}^{\mathfrak{d}'}_{N-1}) \tag{35}$$

Finally, constraints (36)–(38) determine the types of decision variables.

$$\mathcal{N} \in \text{integer} \tag{36}$$

$$\mathcal{X}'^{\mathfrak{d}}_{mjrt}, \mathcal{X}''^{\mathfrak{d}}_{mlrt}, \mathcal{X}'''^{\mathfrak{d}}_{mhrt}, \mathcal{X}_{j'j''t} \in \{0, 1\} \quad \forall \mathrm{m, j, l, h, j', j'', r, t} \tag{37}$$

$$\mathcal{P}^{\mathfrak{d}}_{mjkrt} \mathcal{P}'^{\mathfrak{d}}_{mlkrt} \mathcal{P}''^{\mathfrak{d}}_{mhkrt} \mathcal{Y}'^{\mathfrak{d}}_{pjkt} \mathcal{Y}''^{\mathfrak{d}}_{plkt} \mathcal{Y}'''^{\mathfrak{d}}_{phkt} \mathcal{F}'^{\mathfrak{d}}_{jht} \mathcal{F}''^{\mathfrak{d}}_{lht} \quad \forall \mathrm{m, j, l, h, j', j'', k, r, t} \tag{38}$$

4. Solution methodology

A step-by-step algorithm is proposed in this subsection to solve the proposed method. This algorithm's flowchart is depicted in Fig. 4, which consists of four major steps. The nature of the C-19TKSN problem is dynamic over time due to difficult predictions and changes in the number of C-19 patients. As represented in the flowchart, in the first step, the SPs (i.e., the potential demands relating to different regions of the suspected C-19 cases for various C-19 tests and the prevalence rate of C-19) are generated by using MC simulation. Then, scenarios are redacted by the forward ST construction method. Laporte et al. [10] verified that when the uncertainty of SPs has been progressively realized in each period, the proposed MSSP method is a useful optimization tool.

Furthermore, some of the parameters in this network (e.g., the capacity data for testing centers, opening costs of MTLs, operation costs, transportation costs) are tainted with uncertainty in real-life scenarios due to the dynamic nature of the problem (i.e., possible long-term parameter value fluctuations), which is verified by Mousazadeh et al. [11]. Hence, in the second step, a fuzzy approach based on $\mathcal{M}e$ measure is introduced to deal with uncertainty parameters (i.e., the capacity data for testing centers, opening costs of MTLs, operation costs, transportation costs) in C-19TKSN. In other words, the input parameters are randomly initialized. Then, the uncertainty analysis is performed in the third step, and the amount of confidence level (α) and optimistic–pessimistic parameter (φ) are set up. In the end, a Fuzzy Multi-Objective Goal Programming (FMOGP) is presented to solve the suggested multi-objective model. In other words, the weighted coefficients of the OF are evaluated in the fourth step in order to give DMs an insight into making the preferable trade-off between the aforementioned objectives.

4.1. Multivariate ST generation for SPs

One of the most important issues in a MSSP is generating a ST for SPs that indicates a multivariate stochastic process. The scenario generation scheme is defined in more detail in this section.

4.1.1. Scenario generation

The discretization procedure is called scenario generation for the continuous probability distribution function of SPs from a set of separated scenarios. Monte-Carlo (MC) simulation is used for SPs (i.e., potential demands and the rate of prevalence of C-19) to produce these separated scenarios. An updated first-order autoregressive model, firstly suggested by Sodhi [37], should be added to tackle the high time-variable demands of suspected cases.

In our case, the potential demands of suspected C-19 cases' regions for C-19 tests can be obtained by the following Equation at time t under scenario $\mathfrak{z}$:

$$\mathcal{D}^{\mathfrak{z}}_{mrt} - d'_{mrt} = \delta_{mr}\left(\mathcal{D}^{\mathfrak{z}}_{mr,t-1} - d'_{mr,t-1}\right) + \varepsilon^{N_{\mathfrak{z}}}_{mrt} \tag{39}$$

where δ_{mr} and d'_{mrt-1} are the autoregressive and predetermined parameters, respectively. d'_{mrt-1} is the potential daily demands of suspected C-19 cases' regions dependent on the time, and $\varepsilon^{N_{\mathfrak{z}}}_{mrt}$ is the error parameters with normal distribution, mean and variance zero and δ^2, respectively. The rate of C-19 prevalence is calculated as Eq. (39). A scenario fan is the performance of the MC simulation, including a set of scenarios. We can clarify how to reduce this large number of scenarios in the following parts and turn them into a ST. The rate of prevalence is calculated as above.

4.1.2. Scenario reduction

A large number of scenarios cause a computationally intractable optimization problem. This method, introduced by Dupacova et al. [38], is defined in the following. Assume U is a distribution function of the stochastic $\Im = \left\{\Im^t\right\}_{t=1}^{|T|}$. If U has finite support, then discrete scenarios such that $supp\,(U) = \left\{\Im^1, \Im^2, \ldots, \Im^{|\mathfrak{z}|}\right\}$, $\Im^{\mathfrak{z}} = \left\{\Im^{\mathfrak{z}}_t\right\}_{t=1}^{|T|}$, and $\mathfrak{z} = 1,2,\ldots, |\mathcal{S}|$ can be expressed via $|\mathcal{S}|$. In comparison, $u_{\mathfrak{z}}$ and $\sum_{\mathfrak{z}=1}^{|\mathfrak{z}|} u_{\mathfrak{z}} = 1$ are the corresponding probabilities of the scenarios. Also, let U' 'be a distribution of the same dimension of another stochastic process $\Im' = \left\{\Im'^t\right\}_{t=1}^{|T|}$. Then $SUPP\left(U'\right) = \{\Im'^1, \Im'^2, \ldots, \Im'^{|\mathfrak{z}|}\}$, with $|\mathcal{S}'|$ scenarios and related possibilities $u'_{\mathfrak{z}'}$, $\mathfrak{z}' = 1, 2, \ldots, |\mathcal{S}'|$, and, $\sum_{\mathfrak{z}'=1}^{|\mathfrak{z}'|} u'_{\mathfrak{z}'} = 1$. The optimum solution of the following linear transport problem is the Kantorovich distance (DI^K) between U and, U':

$$DI^K\left(U, U'\right) = \inf\{\sum_{\mathfrak{z}=1}^{|\mathfrak{z}|}\sum_{\mathfrak{z}'=1}^{|\mathfrak{z}'|} \vartheta_{\mathfrak{z}\mathfrak{z}'} C_{|T|}\left(\Im^{\mathfrak{z}}, \Im'^{\mathfrak{z}'}\right) : \vartheta_{\mathfrak{z}\mathfrak{z}'} \geq 0, \sum_{\mathfrak{z}=1}^{|\mathfrak{z}|} \vartheta_{\mathfrak{z}\mathfrak{z}'} = u'_{\mathfrak{z}'}, \sum_{\mathfrak{z}'=1}^{|\mathfrak{z}'|} \vartheta_{\mathfrak{z}\mathfrak{z}'} = u_{\mathfrak{z}}, \forall \mathfrak{z}\mathfrak{z}' \in \mathcal{S}\} \tag{40}$$

where $C_t\left(\Im^{\mathfrak{z}}, \Im'^{\mathfrak{z}'}\right) = \sum_{k=1}^{t}\left\|\Im^{\mathfrak{z}}_k - \Im'^{\mathfrak{z}'}_k\right\|$, $t = 1, 2, \ldots, |T|$ and $\|.\|$ is a norm over R_n. Hence, $C_{|T|}$ is the distance among scenarios over the planning time.

Assume U' is the reduced probability distribution of $\Im = \left\{\Im^t\right\}_{t=1}^{|T|}$, then discrete U' the support comprises scenarios $\Im' = \left\{\Im'^t\right\}_{t=1}^{|\overline{T}|}|$, and $\mathfrak{z}' \in \left\{1, \ldots, \left|\mathcal{S}'\right|\right\} \backslash \mathcal{DS}$ where the set of deleted scenarios is $\mathcal{DS}$. Dupacová et al. [36] has pointed out the minimum distance between U and U' for a fixed range of $\mathcal{DS} \subset \{1, 2, \ldots, |\mathcal{S}|\}$ can be captured by:

$$DI^K\left(U, U'\right) = \sum_{\mathfrak{z}\in\mathcal{DS}} u_{\mathfrak{z}} \min_{\mathfrak{z}'\notin\mathcal{DS}} C_{|T|}\left(\Im^{\mathfrak{z}}, \Im'^{\mathfrak{z}'}\right) \tag{41}$$

And probabilities $u'_{\mathfrak{z}'}$ for U', scenarios, i.e., the retained scenarios $\Im^{\mathfrak{z}'}$, $\mathcal{S}' \notin \mathcal{DS}$, are provided by $u'_{\mathfrak{z}'} = u_{\mathfrak{z}'} + \sum_{\mathfrak{z}\in\mathcal{DS}_{\mathfrak{z}'}} u_s$ where $\mathcal{DS}_{s'} = \{s \in \mathcal{DS}: s' = s'(s)\}$, and $s'(s)$ is a selection of the index set of the closest scenarios to $\Im^{\mathfrak{z}}$, $\forall \mathfrak{z} \in \mathcal{DS}$, i.e. $\mathfrak{z}' = \mathfrak{z}'(\mathfrak{z}) \in \arg\min_{\mathfrak{z}'\notin\mathcal{DS}} C_{|T|}\left(\Im^{\mathfrak{z}}, \Im'^{\mathfrak{z}'}\right), \forall \mathfrak{z} \in \mathcal{DS}$.

We can solve the following reduction problem to choose the set $\mathcal{DS}$ with fixed cardinality $\#\,\mathcal{DS}$ optimally:

$$min\{\sum_{\mathfrak{z}\in\mathcal{DS}} u_{\mathfrak{z}} \min_{\mathfrak{z}'\notin\mathcal{DS}} C_{|T|}\left(\Im^{\mathfrak{z}}, \Im'^{\mathfrak{z}'}\right) \mathcal{DS} \subset \{1, 2, 3, \ldots, |\mathcal{S}|\}, \#\mathcal{DS} = |\mathcal{S}| - \mathcal{NS}\} \tag{42}$$

Where the number of retained scenarios after reduction is $= |\mathcal{S}| - \#\mathcal{DS}$. However, it can be resolved tractably in special cases where $\#\mathcal{DS} = 1$ (eliminating one scenario) and $\#\mathcal{DS} = |\mathcal{S}| - 1$ (maintaining one scenario). Two heuristic methods called forward and backward reduction were developed by [37]. In the backward scenario reduction method, the optimal deletion of one scenario should be replicated recursively before the deletion of $|\mathcal{S}| - \mathcal{NS}$ scenarios, whereas in the forward scenario selection method, the optimal selection of one scenario should be repeated recursively until the $\mathcal{NS}$ scenario is reached. Refer to Heitsch and Romisch [39], Heitsch and Romisch [40], and Dupacova et al. [38] for more information.

4.1.3. ST construction

As described, a form of scenario fan consists of generated scenarios for SPs. In this sub-section, we change the generated scenario fan into a representative ST based on Heitsch

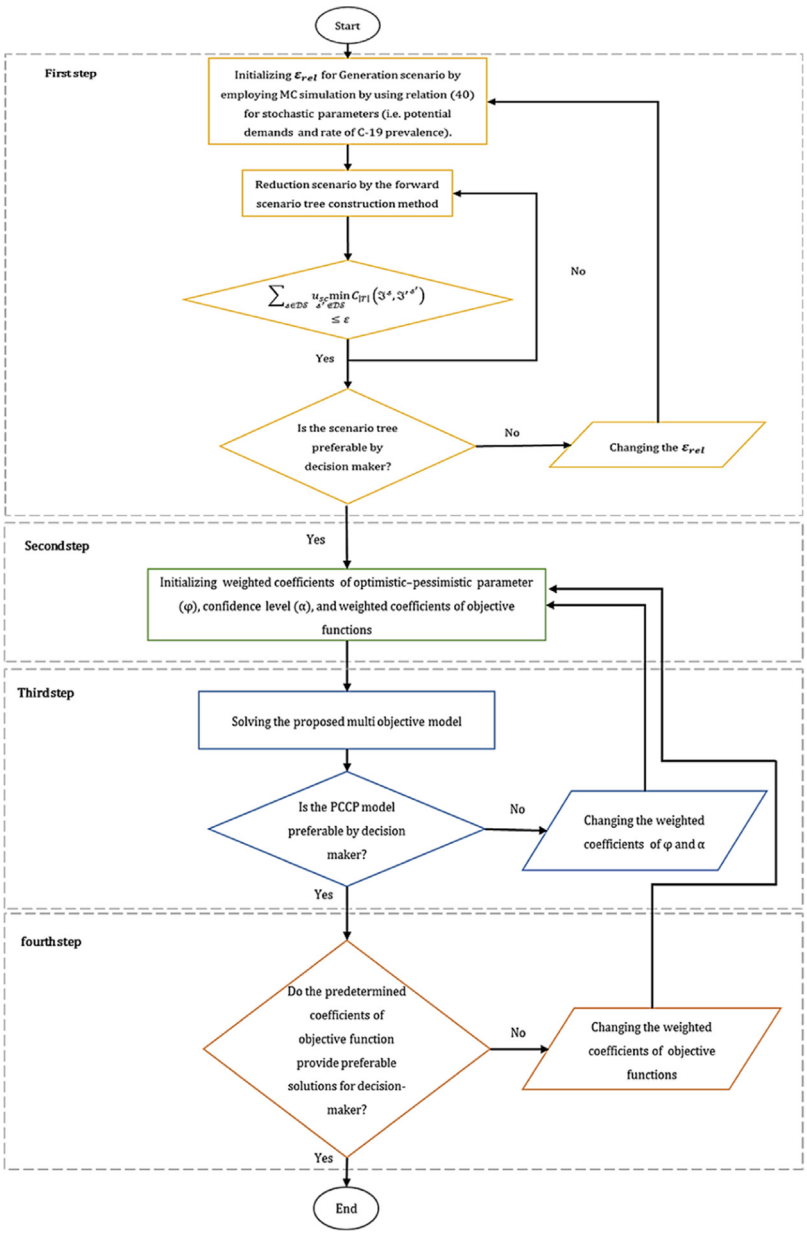

Fig. 4. Flowchart of the proposed methodology for concerned C-19TKSN.

and Romisch [40]. We will reduce the sum of scenarios by the procedure mentioned in sub Section 4.1.2.

We should consider each scenario $\mathfrak{s} = 1, \ldots, |\mathcal{S}|$, as $\Im^{\mathcal{S}} = (\Im^{\mathfrak{s}}_1, \Im^{\mathfrak{s}}_2, \ldots, \Im^{\mathfrak{s}}_{|T|})$ with probability u_{sc}, where $|T|$ is the number of periods for a scenario fan with the probability distribution U connected to the multivariate scenarios. Because all scenarios in the initial node are the same, i.e., $\Im^1_0 = \Im^2_0 = \cdots = \Im^{|\mathcal{S}|}_0 = \Im^*_0$, the total number of existing nodes in the scenario fan is $|\mathcal{S}|\ |T|+1$. The U_ε probability distribution ST would also have a root node of $\Im^*_0$. Also, in the ST, the number of nodes is less than the scenario fan and $DI^K(U, U_\varepsilon) < \varepsilon$.

The forward scenario reduction method is applied in this paper for each period and converting the scenario fan into a ST by successive clustering of scenarios. This method is called the tree construction method of the forward scenario. Readers can Refer to Heitsch and Romisch [40] and Growe-Kuska et al. [41] for more information. For the implementation of the scenario reduction process under the conditional $\sum_{t=1}^{|T|} \varepsilon_t \leq \varepsilon$, ε_t is known to provide a ST with $DI^K(U, U_\varepsilon) < \varepsilon$, at each time t. In other words, in each time t with $\sum_{\mathfrak{s}\in\mathcal{D}\mathcal{S}} u_{sc} \min_{\mathfrak{s}'\notin\mathcal{D}\mathcal{S}} C_{|T|}\left(\Im^{\mathfrak{s}}, \Im'^{\mathfrak{s}'}\right) \leq \varepsilon$, we apply the maximum reduction method. In addition, the distance between both of the two scenarios is determined in each period t using $C_t\left(\Im^{\mathfrak{s}}, \Im'^{\mathfrak{s}'}\right) = \sum_{k=1}^{t} \left\| \Im^{sc}_k - \Im'^{SC'}_k \right\|$.

As presented by Heitsch and Romisch [40], $\varepsilon = \varepsilon_{max} * \varepsilon_{rel}$ is typically used to calculate ε. $0 < \varepsilon_{rel} < 1$, is a fixed value in this relation, describing a scale for the amount of reduction in the initial fan scenario and ε_{max} is the best distance between the initial scenario fan's probability distribution and one of its scenarios of probability one.

In this paper, ε_t is determined via the following equation for the generation of ST at each t period (44):

$$\varepsilon_t = \frac{\varepsilon}{|T|+1}\left[0.5 + q'\left(1 - \frac{t}{|T|+1}\right)\right] \quad \forall t \tag{43}$$

where $q' \in [0, 1]$ is a constant parameter, which in our implementations is assumed to be 1. It can obviously be seen, according to reference (27), that $\sum_{t=1}^{|T|} \varepsilon_t = \frac{\epsilon}{|T|+1}\left[\frac{|T|}{2} + q'(\frac{|T|}{2})\right]$ and as a result, because of $q' \in [0, 1]$, we have $\sum_{t=1}^{|T|} \varepsilon_t \leq \varepsilon$. Besides, if we set $q' = 1$ then, $\sum_{t=1}^{|T|} \varepsilon_t = \frac{|T|}{|T|+1}\varepsilon$.

4.2. Fuzzy programming method (FPM)

FPM can properly control cognitive uncertain data and flexibility in objectives or constraints. FPM can be classified into two main categories: (a flexible programming (FP) b) possibilistic programming (PP). PP is used if we cope with EU in input data according to the unavailability or inadequacy of needed data. In this situation, with both the available objective data and DMs' subjective opinions, a possible distribution is set for each inaccurate data.

Some of the network problem parameters (e.g., facility capacity parameters at different levels of the network, purchase costs of MTLs, transportation cost, operation cost) have a high degree of uncertainty in reality, which is due to the dynamic problem nature [16]. Considering the abovementioned definitions, we can use fuzzy planning approaches based on $\mathcal{Me}$ measurement to describe the proposed model uncertainty in parameters.

4.2.1. Possibilistic chance-constrained programming

One of the most common PP methods is possibilistic chance-constrained programming (PCCP) to deal with the possibility in data. This method has the ability to manage the possibilistic chance constraints that involve the possibilistic data in either the left-hand or right-hand side or both of them. The confidence level (α) should be minimized for the DMs to satisfy the chance constraints by the suggested method. The Possibility ($\mathcal{Pos}$) and Necessity ($\mathcal{Nes}$) are two known fuzzy measures for estimating such assurances in PCCP models [42]. The $\mathcal{Pos}$ measure shows the most optimistic possibility level of possibilistic data happening. In contrast, the $\mathcal{Nes}$ measure enables the minimum (i.e., the most pessimistic) possibility level according to a DM pessimistic attitude. Considering the trapezoidal fuzzy number $\xi = (r_1, r_2, r_3, r_4)$ and $r_1 < r_2 < r_3 < r_4$, the membership function is specified as follows:

$$\mu(x) = \begin{cases} \dfrac{x - r_1}{r_2 - r_1} & \text{if } r_1 \leq x \leq r_2 \\ 1 & \text{if } r_2 \leq x \leq r_3 \\ \dfrac{r_4 - x}{r_4 - r_3} & \text{if } r_3 \leq x \leq r_4 \\ 0 & \text{if otherwise} \end{cases} \tag{44}$$

For $\alpha > 0.5$, the crisp counterparts of membership functions in the measures of $\mathcal{Nes}$ and, $\mathcal{Pos}$ are calculated as follows (Inuiguchi and Ram ık [43], Liu and Iwamura [44]):

$$\mathcal{Pos}\left\{\tilde{\mathrm{i}} \leq x\right\} \geq \alpha \Longleftrightarrow \frac{x - r_1}{(r_2 - r_1)} \geq \alpha$$
$$\Longleftrightarrow x \geq (1 - \alpha)\, r_1 + \alpha r_2 \tag{45}$$
$$\mathcal{Pos}\left\{\tilde{\mathrm{i}} \geq x\right\} \geq \alpha \Longleftrightarrow \frac{r_4 - x}{(r_4 - r_3)} \geq \alpha$$
$$\Longleftrightarrow x \leq \alpha r_3 + (1 - \alpha)\, r_4. \tag{46}$$
$$\mathcal{Nes}\left\{\tilde{\mathrm{i}} \leq x\right\} \geq \alpha \Longleftrightarrow \frac{x - r_3}{(r_4 - r_3)} \geq \alpha$$
$$\Longleftrightarrow x \geq (1 - \alpha)\, r_3 + \alpha r_4 \tag{47}$$
$$\mathcal{Nes}\left\{\tilde{\mathrm{i}} \geq x\right\} \geq \alpha \Longleftrightarrow \frac{r_2 - x}{(r_2 - r_1)} \geq \alpha$$
$$\Longleftrightarrow x \leq \alpha r_1 + (1 - \alpha)\, r_2 \tag{48}$$

Also, for $r_1 > 0$, the expected value of the mentioned measures is described, according to Liu and Liu [45]:

$$\mathrm{E}^{\mathcal{Pos}}[\mathrm{I}] = \int_0^{+\infty} \mathcal{Pos}\{\mathrm{I} \geq x\}\, \mathrm{d}x - \int_{-\infty}^{0} \mathcal{Pos}\{\mathrm{I} \leq x\}\, \mathrm{d}x = \frac{r_3 + r_4}{2} \tag{49}$$

$$\mathrm{E}^{\mathcal{Nes}}[\mathrm{I}] = \int_0^{+\infty} \mathcal{Nes}\{\mathrm{I} \geq x\}\, \mathrm{d}x - \int_{-\infty}^{0} \mathcal{Nes}\{\mathrm{I} \leq x\}\, \mathrm{d}x = \frac{r_1 + r_2}{2} \tag{50}$$

The above interventions are too extreme, although the DMs have a more neutral attitude towards the possibilistic data. To generate a balance between optimistic attitude (OA) and pessimistic attitude (PA) based on experts' opinions, the $\mathcal{Me}$ measure is therefore introduced by Xu & Zhou [46]. Suppose that $\mathcal{A}$ is a fuzzy set in the possibility of space. The $\mathcal{Me}$ measure of $\mathcal{A}$ is stated as follows:

$$\mathcal{Me}[\xi] = \varphi.\mathcal{Pos}\{\mathcal{A}\} + (1 - \varphi).\mathcal{Nes}\{\mathcal{A}\} = \mathcal{Nes}\{\mathcal{A}\}$$
$$+ \varphi\,(\mathcal{Pos}\{\mathcal{A}\} - \mathcal{Nes}\{\mathcal{A}\}) \tag{51}$$

where φ $(0 < \varphi < 1)$ the optimistic–pessimistic data shows the DM's composed attitude. It should be mentioned that $\mathcal{Pos}$ and $\mathcal{Nes}$ measures are particular cases of $\mathcal{Me}$, as follows:

- When $\varphi = 1$, it shows that the DMs have the most OA, so $\mathcal{Me} = \mathcal{Pos}$ shows the maximum chance that even $\mathcal{A}$ holds the possibilistic;
- When $\varphi = 0$, it shows that the DMs have the most PA, so $\mathcal{Me} = \mathcal{Nes}$ shows the minimum chance that even $\mathcal{A}$ holds the possibilistic;

It is suitable for making decisions problem in real-life in a fuzzy environment. In this method, DMs have the ability to take any point across the spectrum of extreme attitudes by using a convex. The $\mathcal{Me}$ measure is calculated as follows:

$$\mathcal{Me}\left\{\tilde{\mathrm{i}} \leq x\right\} = \begin{cases} 0 & \text{if } x \leq r_1 \\ \varphi \times \dfrac{x - r_1}{r_2 - r_1} & \text{if } r_1 \leq x \leq r_2 \\ \varphi & \text{if } r_2 \leq x \leq r_3 \\ \varphi + (1 - \varphi)\, \dfrac{x - r_3}{r_4 - r_3} & \text{if } r_3 \leq x \leq r_4 \\ 1 & \text{if } x \geq r_4 \end{cases} \tag{52}$$

$$\mathcal{Me}\left\{\tilde{\mathrm{i}} \geq x\right\} = \begin{cases} 1 & \text{if } x \leq r_1 \\ \varphi + (1 - \varphi) \times \dfrac{r_2 - x}{r_2 - r_1} & \text{if } r_1 \leq x \leq r_2 \\ \varphi & \text{if } r_2 \leq x \leq r_3 \\ \varphi \times \dfrac{r_4 - x}{r_4 - r_3} & \text{if } r_3 \leq x \leq r_4 \\ 0 & \text{if } x \geq r_4 \end{cases} \tag{53}$$

$$\mathrm{E}^{\mathcal{Me}}[\mathrm{I}] = \int_0^{+\infty} \mathcal{Me}\{\mathrm{I} \geq x\}\, \mathrm{d}x - \int_{-\infty}^{0} \mathcal{Me}\{\mathrm{I} \leq x\}\, \mathrm{d}x$$
$$= \frac{1 - \varphi}{2}(r_1 + r_2) + \frac{\varphi}{2}(r_3 + r_4) \tag{54}$$

In nearly all critical issues which are extremely sensitive to the value of uncertain data, such as healthcare problems, DMs aim to meet the possibilistic chance constraints with a logically high chance. To do so, they utilize a PA for the problem. Hence, φ takes values less than 0.5 to come closer to the $\mathcal{Nes}$ measure to show the DMs' PA. For (φ <0.5), it is calculated as follows:

$$\mathcal{Me}\left\{\tilde{\mathrm{i}} \leq x\right\} \geq \alpha \Longleftrightarrow \varphi + (1 - \varphi)\, \frac{x - r_3}{(r_4 - r_3)} \geq \alpha$$

$$\iff x \geq \frac{(\alpha-\varphi)\, r_4 + (1-\alpha)\, r_3}{1-\varphi} \tag{55}$$

$$\mathcal{M}e\left\{\tilde{\mathrm{i}} \geq x\right\} \geq \alpha \iff \varphi + (1-\varphi)\frac{r_2 - x}{(r_2 - r_1)} \geq \alpha$$

$$\iff x \leq \frac{(\alpha-\varphi)\, r_1 + (1-\alpha)\, r_2}{1-\varphi}. \tag{56}$$

Note: For both αs equal to or greater than 0.5, the crisp counterparts of both $\mathcal{M}e\left\{\tilde{\mathrm{i}} \leq x\right\} \geq \alpha$ and, $\mathcal{M}e\left\{\tilde{\mathrm{i}} \geq x\right\} \geq \alpha$ should be piecewise functions and would not usually fit into one equation, unlike $\mathcal{P}os$, $\mathcal{N}es$ measurements. See Mousazadeh et al. [11] for more information. The compact model (excluding the second OF) is indicated:

$$\mathcal{M}in\ \mathcal{Z} = \mathcal{C}'.\mathcal{Y}$$

Subject to

$$\mathcal{X} \leq \mathcal{W}.\mathcal{Y}$$
$$\mathcal{L}.\mathcal{X} \geq d$$
$$\mathcal{V}.\mathcal{X} = 0$$
$$\mathcal{H}.\mathcal{Y} \leq 1$$
$$\mathcal{X} \leq \mathcal{M}.\mathcal{P}$$
$$\mathcal{G}.\mathcal{P} \leq 1$$
$$\mathcal{P}, \mathcal{Y} \in \{0, 1\}, X \geq 0, \tag{57}$$

$\mathcal{C}'$ is equal to the purchasing MTLs cost, the coefficient matrices of the constraints are the $\mathcal{W}$, $\mathcal{L}$, $\mathcal{V}$, $\mathcal{H}$, and $\mathcal{G}$ matrices, while $\mathcal{M}$ is a large number. Also, vectors $\mathcal{Y}$ and $\mathcal{P}$ indicate the binary variables, whereas vector $\mathcal{X}$ shows the positive continuous variables. In the compact formulation, the second OF is omitted without loss of generality, so it can be acted similarly to the first OF. We convert the possibilistic OF to its crisp counterpart to form the PCCP model by the expected value operator, and the $\mathcal{M}e$ measure is used to deal with the possibilistic constraints of chance, comprising imprecise parameters. Assume $\mathcal{C}'$, $\mathcal{W}$ and d are subject to EU. The formulation of the PCCP is thus determined as:

$$\mathcal{M}in \quad \mathrm{E}[\mathcal{Z}] = \mathrm{E}[\widetilde{\mathcal{C}'}].\mathcal{Y}$$

Subject to

$$\mathcal{M}e\{X \leq \widetilde{\mathcal{W}} \cdot \mathcal{Y}\} \geq \alpha$$
$$\mathcal{M}e\{\mathcal{L}\mathcal{X} \geq \widetilde{d}\} \geq \beta$$
$$\mathcal{V} \cdot \mathcal{X} = 0$$
$$\mathcal{H} \cdot \mathcal{Y} \leq 1$$
$$\mathcal{X} \leq \mathcal{M} \cdot \mathcal{P}$$
$$\mathcal{G} \cdot \mathcal{P} \leq 1$$
$$\mathcal{P}, \mathcal{Y} \in \{0, 1\}, X \geq 0 \tag{58}$$

By placing the equivalent of the expected value in the target function and the $\mathcal{M}e$ measure in the chance constraints, the above model is defined as follows:

$$\mathcal{M}in \quad \mathrm{E}[\mathcal{Z}] = \left[\frac{1-\varphi}{2}\left(\mathcal{C}'_{(1)} + \mathcal{C}'_{(2)}\right) + \frac{\varphi}{2}\left(\mathcal{C}'_{(3)} + \mathcal{C}'_{(4)}\right)\right].\mathcal{Y}$$

Subject to

$$\mathcal{X} \leq \left[\frac{(\alpha-\varphi)\mathcal{W}_{(1)} + (1-\alpha)\mathcal{W}_{(2)}}{1-\varphi}\right] \cdot \mathcal{Y}$$
$$\mathcal{L}\mathcal{X} \leq \left[\frac{(\beta-\varphi)d_{(4)} + (1-\beta)d_{(3)}}{1-\varphi}\right]$$
$$\mathcal{V} \cdot \mathcal{X} = 0$$
$$\mathcal{H} \cdot \mathcal{Y} \leq 1$$
$$\mathcal{G} \cdot \mathcal{P} \leq 1 \tag{59}$$

4.3. FMOGP

Different approaches for solving multi-objective mathematical programming problems have already been presented, which the fuzzy programming approaches are the most common ones [47]. Estimation of a satisfaction level for each OF is one of the most critical reasons for expanding these methods [48]. In this paper, for solving the multi-objective model, the FMOGP method is applied [49]. This method is usually used to deal with the fuzziness of data input in a multi-objective problem, reduce the information needed by DMs to prevent ignorant decisions related to lacking information, and decrease the iterations to reach a preferred solution rapidly [50].

Five phases can be applied according to this method. The first phase is used to evaluate each objective's positive and negative ideal solutions. For each objective, a membership function is evaluated in the second phase. In the third phase, given the constraints, the weighted total of the greatest level of satisfaction of each objective is optimized. By introducing an additional constraint in each phase to avoid deterioration of the solutions, the fourth phase integrates goal programming into the method [51]. In the fifth phase, according to the preferences of DM, the best solution for each objective is obtained. In brief, the algorithm of this fuzzy method is described as follows:

Phase 1: Positive ideal solutions ($\mathcal{PIS}$) and negative ideal solutions ($\mathcal{NIS}$) are calculated. By optimizing the problem, considering only one of the OFs at any time, and ignoring the others, $\mathcal{PIS}$ are obtained. The $\mathcal{NIS}$ are then evaluated, as shown in (60).

$$\mathcal{Z}_1^{\mathcal{NIS}} = \mathcal{Z}_1\left(x_2^{\mathcal{PIS}}\right)$$
$$\mathcal{Z}_2^{\mathcal{NIS}} = \mathcal{Z}_2\left(x_1^{\mathcal{PIS}}\right) \tag{60}$$

Phase 2: A membership function for each OF is defined by (61)–(62) using the definition of fuzzy sets. According to the following formula, $\mu_k(x)$ represents the degree of satisfaction of the k^{th} OF. Note that $\mu_1(x)$ and $\mu_2(x)$ are used for minimization.

$$\mu_1(x) = \begin{cases} 1 & if\, \mathcal{Z}_1 < \mathcal{Z}_1^{\mathcal{PIS}} \\ \dfrac{\mathcal{Z}_1^{\mathcal{PIS}} - \mathcal{Z}_1}{\mathcal{Z}_1^{\mathcal{NIS}} - \mathcal{Z}_1^{\mathcal{PIS}}} & if\, \mathcal{Z}_1^{\mathcal{PIS}} < \mathcal{Z}_1 < \mathcal{Z}_1^{\mathcal{NIS}} \\ 0 & if\, \mathcal{Z}_1 > \mathcal{Z}_1^{\mathcal{NIS}} \end{cases} \tag{61}$$

$$\mu_2(x) = \begin{cases} 1 & if\, \mathcal{Z}_2 < \mathcal{Z}_2^{\mathcal{PIS}} \\ \dfrac{\mathcal{Z}_2^{\mathcal{PIS}} - \mathcal{Z}_2}{\mathcal{Z}_2^{\mathcal{NIS}} - \mathcal{Z}_2^{\mathcal{PIS}}} & if\, \mathcal{Z}_2^{\mathcal{PIS}} < \mathcal{Z}_2 < \mathcal{Z}_2^{\mathcal{NIS}} \\ 0 & if\, \mathcal{Z}_2 > \mathcal{Z}_2^{\mathcal{NIS}} \end{cases} \tag{62}$$

Phase 3: The model is turned into a crisp mixed-integer linear programming (63). The purpose of the model is to optimize a maximum degree of satisfaction in order to satisfy the constraints (i.e., γ)

$$Max\gamma$$

Subject to

$$\mu_k(x) \geq \gamma \quad k = 1, 2$$
$$\gamma \epsilon [0, 1] \tag{63}$$

Nevertheless, the FMOGP is described in equation (64), where "w_k"is the weighted coefficient defined by the DM of the k^{th} OF ($\sum_k w_k = 1$).

$$Max \sum_k w_k \gamma_k$$

Subject to

$$\mu_k(x) \geq \gamma_k \quad \forall k$$
$$\gamma_K \epsilon [0, 1] \tag{64}$$

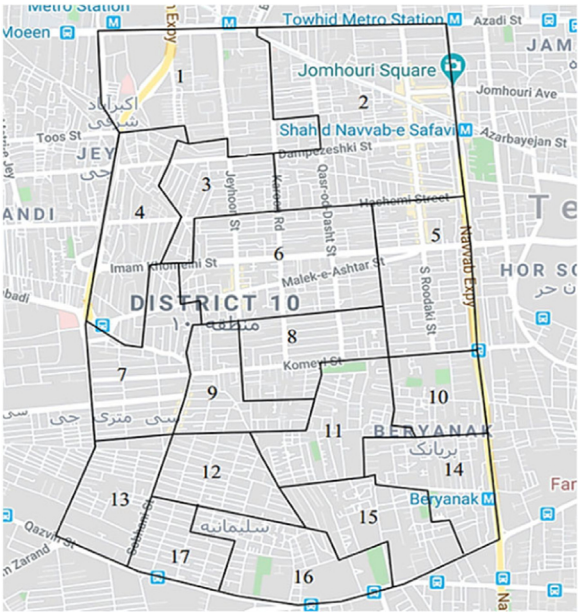

Fig. 5. The regions of district 10 in Tehran.

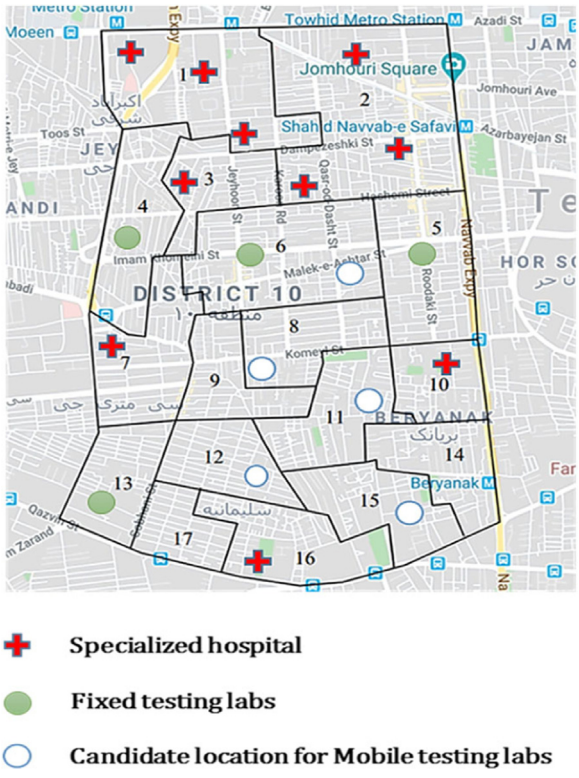

Fig. 6. Location of the concerned laboratories centers and specialized hospitals.

Phase 4: Since solving the model in phase 3 and achieving the results (i.e., z_k^{PJS}), the following model (i.e., (65)) is resolved by presenting a new constraint for each "k" in each phase to obtain the new result (i.e., z_k^{new}), which is calculated as follows and incorporates goal programming with fuzzy set theory ($\gamma_k^{new} \geq \gamma_k or z_k^{new} \leq z_k^{PJS}$).

$$
\begin{aligned}
&Max \sum_k w_k \gamma_k \\
&Subject\ to \\
&\mu_k(x) \geq \gamma_k \quad \forall k \\
&\gamma_k^{new} \geq \gamma_k (or z_k^{new} \leq z_k^{PJS}) \quad \forall k \\
&\gamma_k \epsilon [0, 1] \qquad (65)
\end{aligned}
$$

Phase 5: By repeating the previous phase, decide the best "γ" or "z^{PJS}" by DMs and produce a trade-off between objectives functions.

5. Case description

In this section, we present a real case study to evaluate the validity of the suggested model in practice. We considered Jeyhoon as a case study, which is one of the populated districts in Tehran city. As shown in Fig. 5, the Iran ministry of health and medical education (MoHME) separates this part of the city into 17 blocks; each of them is considered a suspected C-19 cases region. As shown in Fig. 6, established hospitals are in blocks 1, 2, 3, 7, 10, and 16, and established FTLs are in blocks 4, 5, 6, and 13 are in the Jeyhoon area. Blocks 6, 8, 11, 12, and 15 are also considered candidate locations for MTLs, while population, Geographical location, and population density of each region are considered as the main factors for locating the candidates.

For this problem, we collected the necessary data from a key C-19 institution. Also, the three key references we used to obtain the required data for the case study, these necessary data are specific local reports, the expertise of field experts, and reliable records from the hospitals of Tehran. Technical and monetary values are included in the data. For example, uncertain demand and the prevalence rate of each region, the number of kits sent to each center, etc., are required. In addition, the expense of C-19TKSN, including the cost of establishment of MTLs, transportation cost of kits, kits production cost, purchasing cost of MTLs, operation cost, etc., are monetary details measured by dollars.

It should be noted that there are pre-established specialized hospitals and FTLs in the city, but there is no pre-established MTLs, and we want to locate these MTLs for better access for people in the regions and reduce the rate of coronavirus outbreak. In Table 1, the list of regions for hospitals and FTLs has the opportunity to perform C-19 diagnostic tests in Tehran. The population and the area of each block (i.e., suspected C-19 cases' regions) are shown in Table 1, which are considered as the basis for predicting the number of suspected C-19 cases to MTLs, FTLs, and specialized hospitals. The list of hospitals and laboratories' names in Tehran's 10th district is given in Table C.2 in Appendix C.

Arrival time (i.e. rth day) the highest number of people for testing, PCR, RDT, and ELISA with different modes ranging from 0.1 to 5 days, 0.1 to 5, 8.1 to 14, and standard deviation of 0.5 to 5 for each of the test kits, respectively. According to the mode and standard deviation, the number of false-negative results can be calculated with the proposed gamma formula. Notably, the data related to the potential daily demands of suspected C-19 cases' regions were generated based on the hospitals in the Jeyhoon area under uniform distribution performance and the range of [800,200]. For more detail about characteristics of parameters for stochastic parameter generation refer to Table C.1, in Appendix C. Costs of transportation are calculated by using fuel cost and travel time between nodes. Table 2 shows the values of other parameters extracted from MoHME and related papers.

The above points clearly explain the methodology of gathering stochastic data. As mentioned earlier, due to possible fluctuations in some of the network problem parameters (e.g., facility capacity parameters at different levels of the network, purchase costs of MTLs, transportation cost, operation cost) over the long-term

Table 1
The properties of each suspected C-19 cases' region.

Suspected C-19 cases' regions	Population	Area (km^2)
1	21486	0.63
2	23059	1.16
3	11346	0.33
4	13829	0.34
5	20677	0.52
6	40000	0.81
7	16800	0.57
8	19910	0.39
9	20430	0.32
10	20010	0.26
11	20738	0.44
12	14860	0.30
13	13111	0.39
14	18692	0.32
15	16209	0.42
16	7496	0.44
17	18507	0.25
Total	317160	7.89

Table 2
The value of parameters.

Parameters	Value	Reference
The production price of each PCR kit	10$	https://www.sums.ac.ir
The production price of each ELISA kit	6$	https://www.sums.ac.ir
The production price of each RDT kit	3$	https://behdasht.gov.ir
Cost of setting up MTLs	5000$	https://www.wsj.com
Operating cost	50$	https://www.sums.ac.ir

Table 3
Converting deterministic numbers to fuzzy trapezoidal numbers.

Parameters	4 point calculators
Purchasing costs of MTLs	(60%, 90%, 120%, 140%)
transportation cost	(80%, 90%, 100%, 110%)
operation cost	(60%, 90%, 130%, 140%)
Production kits cost	(90%, 95%, 100%, 105%)
Capacity (MTLs)	(60%, 90%, 120%, 140%)
Capacity (FTLs)	(60%, 80%, 120%, 140%)
Capacity (specialized hospitals)	(60%, 90%, 120%, 140%)

horizon, we need to combine these fluctuations in our solution methodology. The experts have recommended that the deterministic data be converted into fuzzy trapezoidal numbers based on four-point percentages that are reported in Table 3. As shown in Table 3, for example, if the crisp estimation of the purchasing costs of MTLs is 10,000$, its fuzzy parameter would be (6000, 9000, 12,000, 14,000).

For the case study, a scenario fan is containing 170 scenarios for the random demand parameter (the SPs) is generated according to the formula presented in Section 4.1, and the reduction of the number of scenarios is converted to the ST. Fig. 7 indicates the obtained ST, which contains eight scenarios. It should be noted that in implementing the method of making the ε_{rel}, we set the $\varepsilon_{rel} = 0.65$.

5.1. Computational results

We present district 10 of the Jeyhoon for our real case study. In this paper, the model is solved via the CPLEX using GAMS software, and a PC with Intel Core i7, CPU 2.8 GHz, and 8 GB of RAM is used for all implementations. According to the results, 5 MTLs have been established in blocks 6, 8, 11, 12, and 15 for optimal supply chain design. Table 4 shows the number of C-19 kit's demands (suspects C-19 cases) assigned to each center in each scenario. Table 5 shows the number of tests with PCR kits, which collects in specialized hospitals consisting of tests in specialized hospitals and kits sent from FTLs and MTLs.

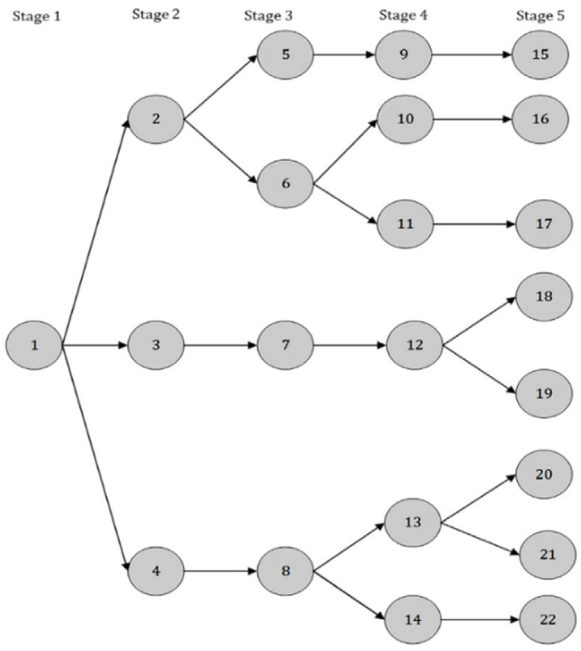

Fig. 7. The scenario tree of the case study.

As shown in Table 4, the number of C-19 kit's demands assigned to MTLs for RDT testing is higher than FTLs and specialized hospitals. Because as mentioned before, RDT tests take less time and its equipment is cheaper. Unlike RDT tests, PCR tests require more expensive equipment, and the number of suspected C-19 people who take PCR tests in MTLs and FTLs, their samples must be sent to specialized hospitals. Therefore, according to the above explanations and Table 5, most of the C-19 kit's demands have been assigned to specialized hospitals. On the other hand, due to the greater and faster availability of ELISA kits, the suggested model has assigned suspicious people to ELISA kits due to the lower probability of error of ELISA kits on the desired day and also the lack of PCR kits.

According to each region's coverage radius, the allocation of the region of suspected C-19 cases to MTLs, FTLs, and specialized hospitals is shown in Fig. 8. Therefore, all regions of suspected C-19 cases are covered by at least one testing center. We have considered the transportation costs according to the traveled distance between nodes (i.e. the cost of transporting people from the regions of suspected C-19 cases to the MTLs, FTLs, and specialized hospitals). Therefore, the model allocates the region to the centers according to the capacity of the desired facility and the cost of sending the suspected C-19 cases to all facilities. Therefore, it is possible for the model to allocate the regions of suspected C-19 cases to a center at a farther distance. In conclusion, all testing centers in the Jeyhoon area are appropriately distributed.

5.1.1. The value of MSSP

Huang and Ahmed [52] represented the relative value of MSSP (RVMS) in a capacity planning optimization problem with uncertain parameters to analyze the values of TSSP and MSSP in terms of the objective function. The RVMS formulation is rendered as follows:

$$\mathcal{AVMS} = \frac{\mathbb{OF}^{\mathcal{TSSP}} - \mathbb{OF}^{\mathcal{MSSP}}}{\mathbb{OF}^{\mathcal{TSSP}}} \times 100 \tag{66}$$

where $\mathbb{OF}^{\mathcal{TSSP}}$ is the TSSP optimal objective value and $\mathbb{OF}^{\mathcal{MSSP}}$ is the MSSP optimal objective value.

Table 4
The number of C-19 kit's demands assigned to each center for $w_1 = 0.33$, $w_2 = 0.67$, $\alpha = 0.9$, $\varphi = 0.1$.

scenarios	PCR kits			RDT test			ELISA kits		
	MTLs	FTLs	Hospital	MTLs	FTLs	Hospital	MTLs	FTLs	Hospital
$\mathcal{S}_1$	0	0	1860	1124	723	1684	42	679	1331
$\mathcal{S}_2$	27	75	1745	840	554	1636	45	744	1060
$\mathcal{S}_3$	41	91	1973	611	606	1982	39	615	1355
$\mathcal{S}_4$	23	46	2145	678	634	2203	77	776	1316
$\mathcal{S}_5$	23	78	2188	586	690	1850	77	718	1261
$\mathcal{S}_6$	0	12	2026	777	891	1514	75	709	1194
$\mathcal{S}_7$	0	30	1881	738	851	1740	61	729	1194
$\mathcal{S}_8$	0	50	2061	800	963	1448	98	613	1305

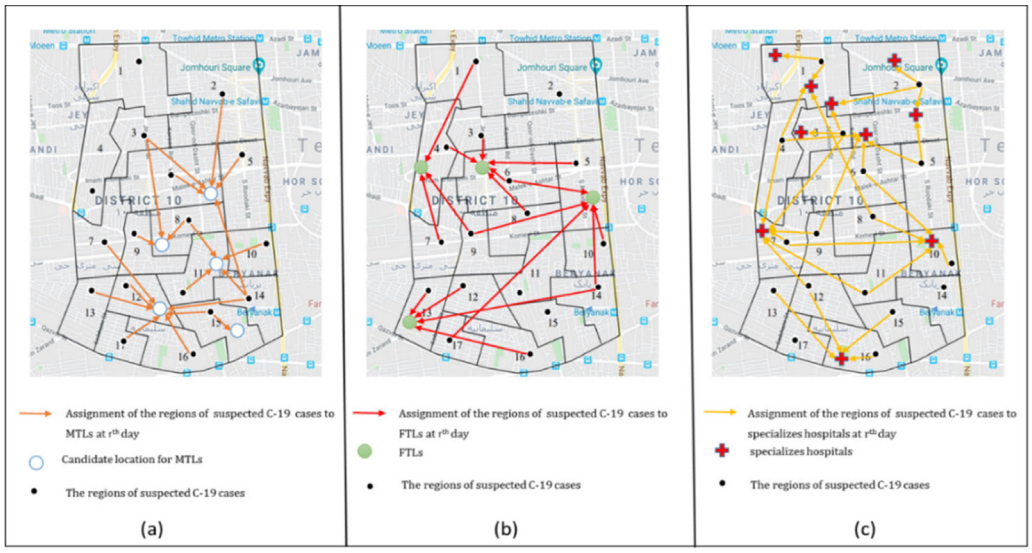

Fig. 8. Assignment of the region of suspected C-19 cases to (a) MTLs, (b) FTLs, and (c) specializes hospital at rth day.

We need an additional type of constraint in the MSSP model, called non-anticipativity constraint that non-anticipativity constraint is presented in Section 3.1 but we do not need non-anticipativity constraint in the TSSP model. Therefore, we want to first distinguish the MSSP model from the TSSP model. The comparison between the two models is shown in Figs. 9 and 10. Assuming there is a stochastic production problem with three time periods and five scenarios. The squares represent the time points for primary allocation decisions, while the triangles represent the time points for possible updates for the allocation decisions. Fig. 9 shows the TSSP model in which all of the primary allocation decisions need to be determined at the beginning of the time horizon $t = 1$ without having any information of uncertainty, and the allocation updates can be made after the realization of uncertainty in the first period. Fig. 10 shows a MSSP in which the primary allocation decisions can be determined at the beginning of each time period based on the previous information. Clearly, the MSSP model has a larger decision space and its primary allocation decisions, as well as allocation updates, are allowed based on the previous realizations and decisions [53].

An important requirement of the non-anticipative decision process is that the primary allocation decisions taken at any point do not depend on future realizations of uncertainty, but it is impacted by the previous realizations of uncertainty as well as the knowledge of previous decisions. We use Fig. 10 to illustrate the functionality of a non-anticipativity constraint in the MSSP model. At the beginning of $t = 1$, no information is revealed, so the primary allocation for $t = 1$ should be identical across all scenarios. During the first time period, uncertainty is revealed to be one of the two outcomes. In Fig. 10, scenarios 1, 2, and 3 share one outcome while scenarios 4 and 5 share the other outcome

Table 5
Number of tests with PCR kits in specialized hospitals for $w_1 = 0.33$, $w_2 = 0.67$, $\alpha = 0.9$, $\varphi = 0.1$.

Scenarios	MTL-hospital	FTL-hospital	hospital	Total
$\mathcal{S}_1$	0	0	1860	1860
$\mathcal{S}_2$	27	75	1745	1647
$\mathcal{S}_3$	41	91	1973	2105
$\mathcal{S}_4$	23	46	2145	2214
$\mathcal{S}_5$	23	78	2188	2289
$\mathcal{S}_6$	0	12	2026	2038
$\mathcal{S}_7$	0	30	1881	1911
$\mathcal{S}_8$	0	50	2061	2111

at time $t = 2$. Given the information in the first time period, the primary allocation decisions should be identical at $t = 2$ for $\mathfrak{s} = 1, 2, 3$ and the same principle applies for $\mathfrak{s} = 4, 5$ and $t = 2$.

According to the above mention, In the TSSP model, we assume the allocation decisions of the regions of suspected C-19 cases to MTLs, FTLs, and specialized hospitals have to be determined in all periods before uncertainty realization as the first stage decisions. It should be mentioned that in dynamic TSSP models, first-stage decisions are made for multiple periods in many studies. To obtain the TSSP, we relax non-anticipativity constraints from the stochastic model and enforce decision variables $\mathcal{X}'^{\mathfrak{s}}_{mjrt}$, $\mathcal{X}''^{\mathfrak{s}}_{mlrt}$ and $\mathcal{X}'''^{\mathfrak{s}}_{mhrt}$ allocation decisions of the regions of suspected C-19 cases to MTLs, FTLs, and specialized hospitals at each period, to have the identical values in all scenarios by adding the constraints (67)–(69):

$$\mathcal{X}'^{\mathfrak{s}}_{mjrt} = \mathcal{X}'^{\mathfrak{s}'}_{mjrt} \quad \forall m, j, r, t \in T(\mathfrak{s}, \mathfrak{s}') \in \mathcal{S} \tag{67}$$

$$\mathcal{X}''^{\mathfrak{s}}_{mlrt} = \mathcal{X}''^{\mathfrak{s}'}_{mlrt} \quad \forall m, l, r, t \in T(\mathfrak{s}, \mathfrak{s}') \in \mathcal{S} \tag{68}$$

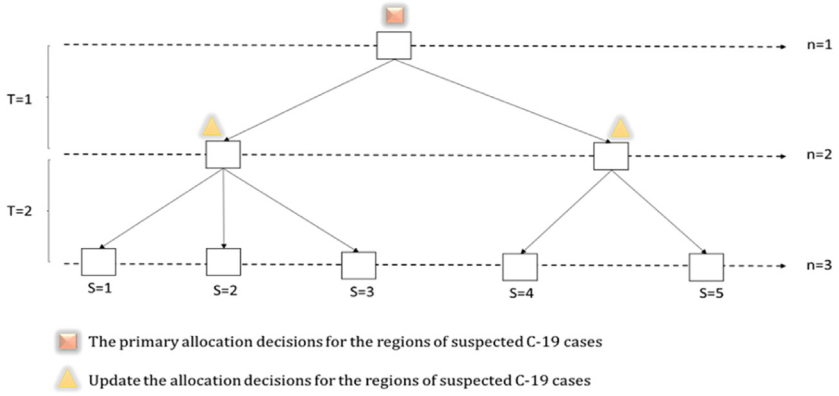

Fig. 9. A scheme of the TSSP.

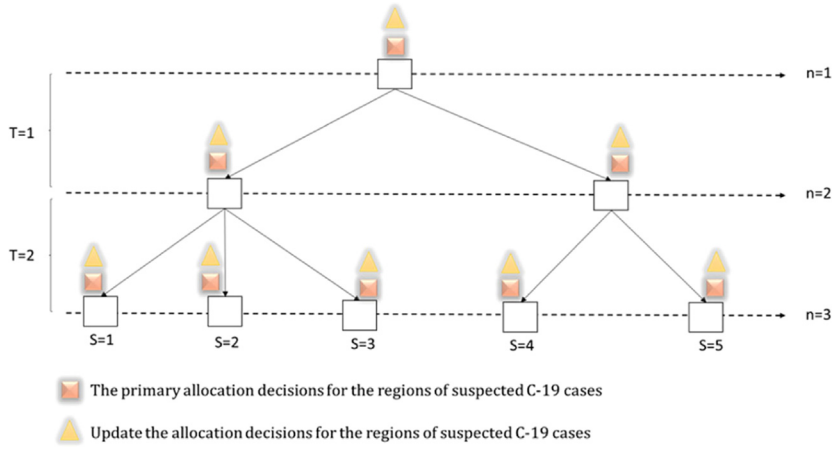

Fig. 10. A scheme of the MSSP.

Table 6
Summary of the results of TSSP and MSSP models for $w_1 = 0.33$, $w_2 = 0.67$, $\alpha = 0.9$, $\varphi = 0.1$.

	TSSP	MSSP	RVMS
OF1 ($)	5.2357E+5	4.7502E+5	9
OF2	88	87	1.1
Number of MTL	5	5	–

$$\mathcal{X}'''^{\mathfrak{z}}_{mhrt} = \mathcal{X}'''^{\mathfrak{z}'}_{mhrt} \quad \forall m, h, r, t \in T(\mathfrak{z}, \mathfrak{z}') \in \mathcal{S} \tag{69}$$

Table 6 presents a summary of the optimal values of the TSSP and MSSP models' objective functions. The purpose of establishing a MTLs is to reduce the prevalence of C-19 and the risk of false results; all 5 MTLs have been established in the MSSP model and have reduced the risk function of false results. In the MSSP model, updating each stage reduces costs (i.e., transportation cost), and the objective function related to the expenses has less value than the TSSP model according to Figs. 11 and 12. Table 6 indicates that the value of the objective function of the TSSP model is significantly greater than the MSSP model. Therefore, we can make meaningful progress by using the MSSP model. In fact, in TSSP, allocation decisions are related to the first-stage decisions, and also, these decisions are not flexible about stochastic events occurring in prior stages.

Table 7 shows the RVMS values for the 4 instances (by changing the problem instance size) to better demonstrate the performance superiority of the MSSP model to TSSP. The RVMS criterion values reported in Table 7 highlight the importance of applying MSSP in our problem setting. We can see from the results that the average RVMS_{OF1} is 8.11%, and by increasing the period count in problem instances, the value of the RVMS_{OF1} increases, relatively.

5.1.2. PCCP method analysis

The role of the suggested PCCP method on the C-19KTSN is examined. Therefore, this model is solved for different values of confidence level (α) and the parameter of optimistic–pessimistic (φ), then the changes in the objective functions are examined. The performance of two OFs is estimated, and the values of each OF are optimized and indicated in Table 8. As shown in Table 8, it can be seen that increasing of α and reducing φ have worse performance; consequently, the values of objective functions take more value. Also, Table 8 displays the gap and computing time of each method. Based on the results, PCCP (a) announces the worst value of cost and risk of false result objectives, and PCCP(c) has the best cost and risk of false result objectives of the network.

In this section, we compare the proposed model's performance under the realization. To do so, from the fuzzy range of imprecise parameters, 30 random data sets are created. The optimal values of decision variables taken in the MSSP model are integrated into a linear programming model described in the model (70). Hence, under each random set for each of the suggested models, model (70) is optimized. As we can see, parameters $\mathcal{X}^*$, $\mathcal{Y}^*$, and $\mathcal{P}^*$ are optimal values of location, allocation, and suspected C-19 cases flow decisions obtained in the MSSP model and are described as an input in this model. Also, S_1 is the newest decision variable in this model, reflecting the number of capacity constraint violations.

Table 7
Investigation of the RVMS for $w_1 = 0.33$, $w_2 = 0.67$, $\alpha = 0.9$, $\varphi = 0.1$.

Instance number	$/M/$, $/T/$	$\lvert\mathcal{S}\rvert$, ε_{rel}	$/H/$,$/L/$,$/J/$	MSSP		TSSP		RVMS	
				OF1 ($)	OF2	OF1 ($)	OF2	$RVMS_{OF1}$	$RVMS_{OF2}$
1	/17/,/4/	|9| , 0, 65	/10 /,/4 /,/5/	3.3929E+5	67	3.5161E+5	69	3.50	2.8
2	/17/,/6/	|8| , 0.65	/10 /,/4 /,/5/	5.9491E+5	105	6.9136E+5	107	13.95	0.95
3	/10/,/4/	|10| , 0, 65	/5 /,/2/,/2/	2.2910E+6	47	2.3977E+5	49	4.4	4.08
4	/10/,/6/	|8| , 0, 65	/5 /,/2/,/2/	3.5338E+5	77	3.9295E+5	78	10.06	1.2

Table 8
The results of the various uncertain model in real data for $w_1 = 0.33$, $w_2 = 0.67$.

model	Parameters	Objective functions		Gap (%)	Time (minutes)
		OF1 ($)	OF2		
PCCP(a)	$\alpha = 1,\ \varphi = 0$	2.6311E+5	91.414	0.00	7:02
PCCP(b)	$\alpha = 0.75,\ \varphi = 0.25$	2.5098E+5	90.685	0.00	6:57
PCCP(c)	$\alpha = 0.5,\ \varphi = 0.5$	2.3885E+5	89.956	0.00	6:18

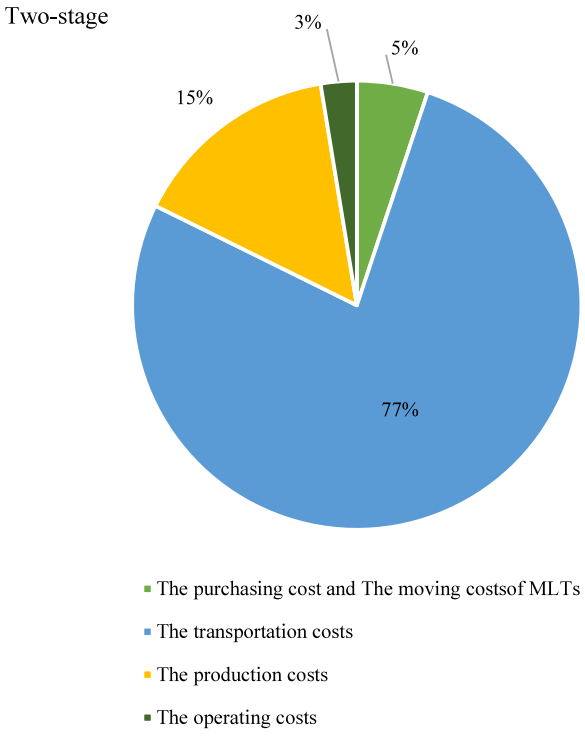

Fig. 11. Optimal costs for the TSSP model.

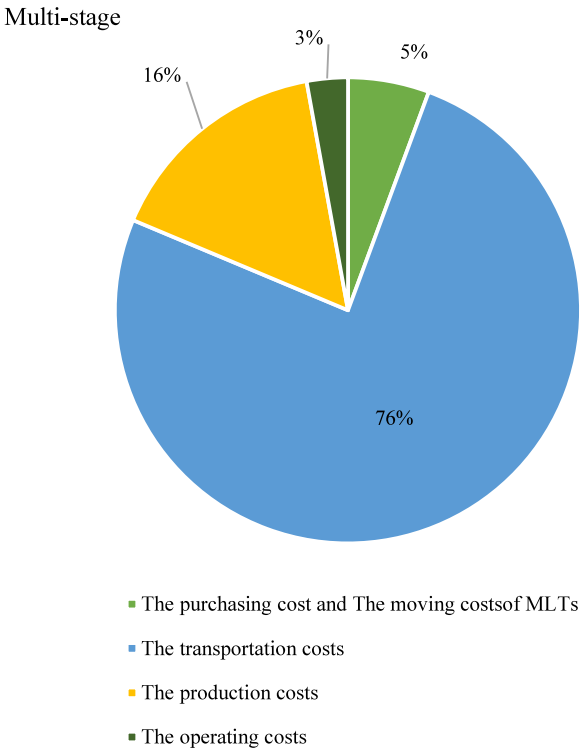

Fig. 12. Optimal costs for the MSSP model.

Furthermore, under model optimization, their values are achieved for only the first OF, that is, $\mathcal{Z}'_1$ since all the terms are fixed in the second OF, that is, $\mathcal{Z}'_2$. We would have a same-scaled measure for evaluating the performance of the suggested model because of the model (70):

$$
\begin{aligned}
&\mathcal{M}in \quad \mathcal{Z}'_1 = \mathcal{C}'_{Real}.\mathcal{Y}^* + \delta_1 S_1\\
&\mathcal{M}in \quad \mathcal{Z}'_2 = \ell'_{Real}.\mathcal{X}^*\\
&S.T.\\
&\mathcal{X}^* \le \mathcal{W}_{Real}.\mathcal{Y}^* + S_1\\
&\mathcal{V}.\mathcal{X}^* = 0\\
&\mathcal{H}.\mathcal{Y}^* \le 1\\
&\mathcal{X}^* \le \mathcal{M}.\mathcal{P}^*\\
&\mathcal{G}.\mathcal{P}^* \le 1\\
&S_1 \ge 0.
\end{aligned}
\tag{70}
$$

Note 1. Since the $\mathcal{Z}'_1$ aims to minimize the decision variable S_1, the minimum possible values that Cause the equality of the left and right-hand sides of these constraints will be their optimal values.

Note 2. In some cases, it can also be reasonable to consider the strategic decisions' optimum values (e.g., location decisions) as an input to the implementation model and optimize other decisions (i.e., the tactical and operational levels).

In the realization stage, three models, each under 30 randomly generated data sets, are implemented, whose results are shown in Table 9. Notably, for each of the proposed models, the average, standard deviation ($\mathcal{SD}$), and coefficient of variance ($\mathcal{CV}$) of the results are presented in Table 9. The PCCP(c) model outperforms other models among the proposed models in terms of the average measure and, rather, the $\mathcal{SD}$ and $\mathcal{CV}$ measures in terms of both first and second objective function.

As reported earlier, most models are extremely sensitive to the value of uncertain data such as healthcare systems, the DMs utilize a PA toward the problem. Therefore, they aim to satisfy

Table 9
The performance of the proposed models under realization for $w_1 = 0.33$, $w_2 = 0.67$.

Model	Parameters	OF1 ($)			OF2		
		Average	SD	CV(SD/average)	Average	SD	CV(SD/average)
PCCP(a)	$\alpha = 1,\ \varphi = 0$	3.597016E+7	8.11E+5	0.02255	89.818	3.48	0.03867
PCCP(b)	$\alpha = 0.75,\ \varphi = 0.25$	3.081596E+7	8.10E+5	0.02629	89.650	3.45	0.03823
PCCP(c)	$\alpha = 0.5,\ \varphi = 0.5$	2.472947E+7	1.21E+5	0.04921	57.506	1.59	0.02764
Deterministic	–	6.472267E+9	3.25E+7	0.00502	87.77	2.46	0.02802

the possibility constraints with a logically high chance that indicates an orientation toward the $\mathcal{N}es$ measure. Consequently, if the proposed fuzzy models (i.e. PCCP models) are ignored and the deterministic model simply resolved under deterministic parameters, the deterministic model should be solved by the most pessimistic values of uncertain parameters, which is exactly the same as solving the PCCP (a) model.

As the DMs are only sensitive to the deviation of the values of the objective function over the expected optimal values and PCCP (c) has the best performance among various versions of the PCCP model, it is suggested to be using PCCP (c) to deal with the problem under investigation. In general, to choose the most suitable version of the PCCP models, some parameters, such as the nature of the problem concerned and DM's expectations, should be considered. However, as mentioned earlier, the most suitable approach for the problem concerned is the PCCP (c). Moreover, Table 9 represents the superiority of PCCP (c) over other presented models in terms of the first objective function.

PCCP (c) is clearly superior to the other two models. The results of the PCCP (c) are compared with the other models using a t-test to confirm that the results differ significantly from those of the other models. Performing a t-test at a significance level of 5% (i.e., $\alpha = 0.05$), the results indicate that the average of objective functions value obtained by the PCCP (c) has a significant difference from the average objective functions values of other models at a confidence level of 95%.

5.1.3. FMOGP analysis

In this part, FMOGP is prepared for solving our suggested C-19TKSN. Fig. 13 displays the FMOGP algorithm's convergence curve. As shown, the maximal γ does not change after two iterations and is equal to 1. Table 10 also displays various examples of the weighted coefficients of the first OF. If the weighted coefficient of the second OF (ω_2) takes more value, the total cost increment. In fact, when the weighted coefficient of the second OF takes more value, more MTLs would be purchased in a decentralized manner to reduce the risk of false results in any scenario. It is occurred due to minimizing the risk of false results.

The examination of the weighted coefficients result of various objectives gives DMs insight into making a preferred tradeoff between the aforementioned objectives according to case-specific purposes.

Table 10
Various examples of the weighted coefficients of objective functions.

Coefficients	OF1 ($)	Gap (%)	Time (minutes)
$w_1 = 0,\ w_2 = 1$	3.1870E+6	0	5:54
$w_1 = 0.1,\ w_2 = 0.9$	5.7843E+5	0	6:55
$w_1 = 0.2,\ w_2 = 0.8$	5.2430E+5	0	6:46
$w_1 = 0.3,\ w_2 = 0.7$	4.7437E+5	0	6:36
$w_1 = 0.4,\ w_2 = 0.6$	4.5863E+5	0	6:42
$w_1 = 0.5,\ w_2 = 0.5$	4.3247E+5	0	6:41
$w_1 = 0.6,\ w_2 = 0.4$	4.1800E+5	0	6:36
$w_1 = 0.7,\ w_2 = 0.3$	4.3780E+5	0	6:35
$w_1 = 0.8,\ w_2 = 0.2$	4.3483E+5	0	6:30
$w_1 = 0.9,\ w_2 = 0.1$	4.2520E+5	0	6:45
$w_1 = 1,\ w_2 = 0$	4.0834E+5	0	5:55

5.1.4. Estimate the amount of false-negative error

In this section, we compare several different instances by changing the standard deviation and mode to show what changes occur in the allocation process in each scenario and the value of the objective function. As mentioned in Section 5, the Mode range (i.e., the maximum number of people who test on day r) of each kit is 0.1 to 5 days, 0.1 to 8, 8.1 to 14, respectively, as well as the standard deviation (dispersion Data from the average), is in the range of 0.5 to 5. By changing the standard deviation and mode, we reach different results. According to the Gamma formula, the formula of shape and rate parameters in Eq. (1)–(3) in Section 3.1, we estimate the number of false results C-19 test. In Table 11, different instances for mode and standard deviation of PCR, RDT, ELISA kits are presented.

A comparison between the number of PCR, RDT, and ELISA kits assigned to suspected C-19 cases with increasing mode and standard deviation of each kit is shown in Figs. 14–16. According to Fig. 14, increasing the standard deviation of PCR kits leads to an increase in the coefficient of sensitivity error (i.e., increasing the number of false-negative results), so the number of false results increases. Performance of RDT kits by increasing in standard deviation is similar to PCR kits, According to Fig. 15. On the other hand, as the mode of the PCR and RDT kits converges to the end of the specified range, the coefficient of sensitivity error decreases, and as a result, the number of false results decreases. In fact, false negatives will be minimized if all suspected C-19 cases go to test centers and test by PCR and RDT kits on the 4th and 5th day with less dispersion; Because the disease is at its peak on the 4th and 5th day and then improves, and the probability of the absence of the virus in the patient's test sample is much lower than on other days.

According to Fig. 16, increasing the standard deviation of ELISA kits leads to a decrease in the coefficient of sensitivity error, so the number of false-negative results decreases. The difference with other C-19 test kits is that the ELISA kit is not performed to diagnose C-19 disease, although the kit shows whether the individual got the virus or not. For this reason, we have maximized the sensitivity error of the Elisa kit in the first 7 days so that suspected C-19 cases will not be assigned to this kit in the first seven days. Therefore, the sensitivity error is decreased by increasing the standard deviation. Also, false-negative results are reduced by increasing the mode of Elisa kits is similar to the standard deviation of ELISA kits. For example, if a suspected C-19 case is tested with Elisa kit on the 14th day, it would have less error than if they are tested with the same kit on day 8.

Table 11
The instance for mode and standard deviation of different C-19 kits.

Test instances	PCR	RDT	ELISA
Instance 1	$\mathcal{M} = 2\ \ \boldsymbol{\sigma} = 1.1$	$\mathcal{M} = 2\ \ \boldsymbol{\sigma} = 1.35$	$\mathcal{M} = 9\ \ \boldsymbol{\sigma} = 3.1$
instance 2	$\mathcal{M} = 2\ \ \boldsymbol{\sigma} = 2$	$\mathcal{M} = 2\ \ \boldsymbol{\sigma} = 1.35$	$\mathcal{M} = 9\ \ \boldsymbol{\sigma} = 3.1$
instance 3	$\mathcal{M} = 4\ \ \boldsymbol{\sigma} = 1.1$	$\mathcal{M} = 2\ \ \boldsymbol{\sigma} = 1.35$	$\mathcal{M} = 9\ \ \boldsymbol{\sigma} = 3.1$
instance 4	$\mathcal{M} = 2\ \ \boldsymbol{\sigma} = 1.1$	$\mathcal{M} = 2\ \ \boldsymbol{\sigma} = 2.5$	$\mathcal{M} = 9\ \ \boldsymbol{\sigma} = 3.1$
instance 5	$\mathcal{M} = 2\ \ \boldsymbol{\sigma} = 1.1$	$\mathcal{M} = 5\ \ \boldsymbol{\sigma} = 1.35$	$\mathcal{M} = 9\ \ \boldsymbol{\sigma} = 3.1$
instance 6	$\mathcal{M} = 2\ \ \boldsymbol{\sigma} = 1.1$	$\mathcal{M} = 2\ \ \boldsymbol{\sigma} = 1.35$	$\mathcal{M} = 9\ \ \boldsymbol{\sigma} = 4$
instance 7	$\mathcal{M} = 2\ \ \boldsymbol{\sigma} = 1.1$	$\mathcal{M} = 2\ \ \boldsymbol{\sigma} = 1.35$	$\mathcal{M} = 14\ \ \boldsymbol{\sigma} = 3.1$

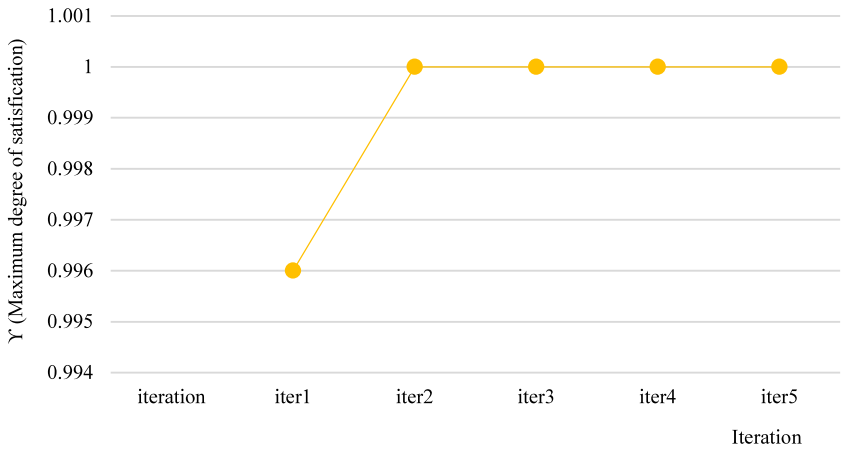

Fig. 13. The FMOGP algorithm Convergence curve.

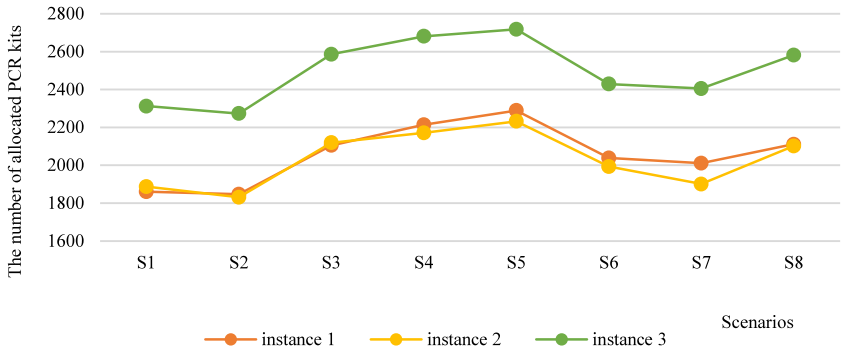

Fig. 14. Comparison of the number of PCR kits allocated to suspected C-19 cases.

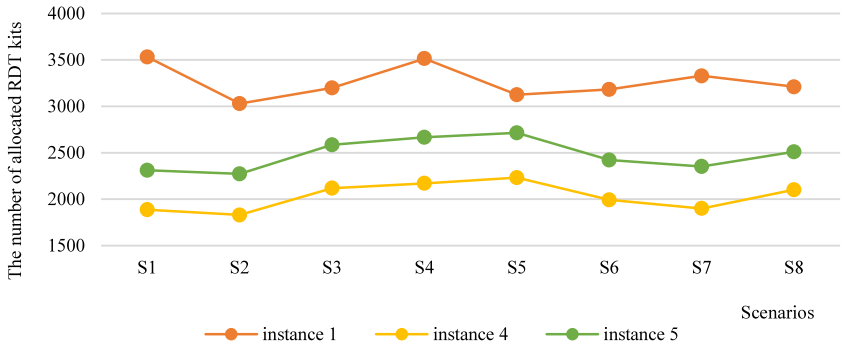

Fig. 15. Comparison of the number of RDT kits allocated to suspected c-19 cases.

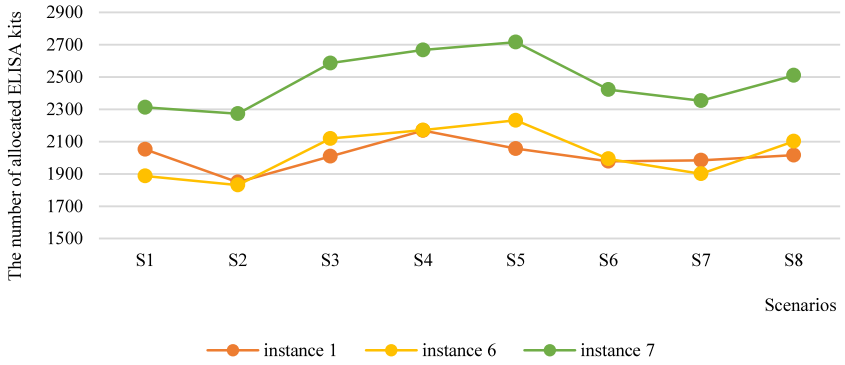

Fig. 16. Comparison of the number of EISA kits allocated to suspected C-19 cases.

Table 12
Sensitivity analysis of the potential demand.

Parameter values	OF1 ($)	OF2
0.95	4.1854E+5	83.108
0.97	4.4600E+5	84.858
1	4.7502E+5	87.482
1.03	4.9282E+5	90.107
1.05	5.1713E+5	91.857

Note: If the sensitivity coefficient error increases and we do not have a limit on the number of production kits, the model assigns suspicious cases to the rest of the kits and may even show a lower total error result but in some countries, the production capacity of the C-19 kits is limited. For this reason, by changing the standard deviation and mode, the model has to assign the suspected C-19 cases to the kit with a high sensitivity coefficient error, thus increasing the number of false-negative results.

5.1.5. Sensitivity analysis

The primary trigger for designing and constructing a network is potential demand. Indeed, a smaller number of existing testing centers will be adequate for the lower levels of demand, while a wider network could be established to meet the high demands. Figs. 17 and 18 display the findings obtained from conducting sensitivity analysis on potential demand parameters. If the size of the demand rises, more facilities can be opened and rising costs. Obviously, the amount of false results is also rising with increasing demand. As can be seen, in Figs. 17 and 18, the equilibrium value of both OFs will concurrently increase as demand for taking the C-19 tests increases. The optimal values of the first OF and second OF are reported in Table 12.

Among the essential parameters whose sensitivity analyses are inevitable are also the opening costs of MTLs. The results of sensitivity tests conducted on the establishment costs of healthcare facilities are achieved in Fig. 19. As can be seen, more MTLs are opened when the model is resolved under the minimum purchasing rate. On the other hand, the total number of MTLs purchased at C-19TKSN is marginally diminished by the rise in purchasing costs. Also, since the model does not have any budget constraints, even when it is solved under a reasonably high-cost value, the model can remain feasible, but the optimal values of the minimum satisfaction levels are gradually reduced.

5.1.6. Key findings

In designing C-19TKSN under uncertainty, the MSSP model has a significant preference over the TSSP model in the sense that if a supply chain takes its decisions considering a MSSP model, then it has more flexibility in terms of changing its decisions based on various uncertain events in every period. Hence, the results indicate that the performance of the MSSP model is remarkably reduced in comparison with the TSSP model regarding the total cost of the supply network and the false results test.

Also, the mode and standard deviation of each C-19 kit show different results based on the time of onset of symptoms. Due to this, increasing the standard deviation of PCR and RDT kits leads to an increase in the coefficient of sensitivity error (i.e., increasing the number of false-negative results), so the number of false results tests increases. On the other hand, as the mode of the PCR and RDT kits increases, the coefficient of sensitivity error decreases, and as a result, the number of false results decreases. Nevertheless, in ELISA kits, it is slightly different from the PCR and RDT kits. In ELISA kits, the sensitivity error decreases with increasing standard deviation and leads to reduce the number of false-negative results. Also, increasing the mode of Elisa Kit due to similar standard deviation reduces false-negative results.

6. Conclusions

In this paper, a MSSP method by using non-anticipatively constraints was suggested for designing a C-19TKCN under uncertainty. Moreover, a MC simulation approach was utilized for achieving a fan of scenarios. By utilizing a forward scenario reduction method, the number of these scenarios were then reduced to construct a proper ST for the SPs. This network consists of suspected C-19 cases, kit manufacturers' centers, FTLs, MTLs, and specialized hospitals.

As mentioned earlier, three methods are available for testing C-19 (i.e., molecular tests, diagnostic tests, and antibody tests), which vary in cost and efficiency. To reduce referrals and reduce congestion in test centers, which can lead to a high prevalence of the C-19 disease, MTLs are provided in some areas to improve access for people and reduce the movement and transportation of people among areas and reduce the prevalence of the C-19 disease. In this paper, we take the optimal strategy to select the appropriate kits based on the time of symptoms of people onset. To this end, this paper aims to reduce false results of C-19 kits by considering proper planning, which incorporates the fundamental characteristics of diagnostic C-19 tests (i.e., specificity and sensitivity). In the sensitivity characteristic, a gamma formula is presented to estimate the error rate of false-negative results in Section 3.1, and in the specificity characteristic, we consider the error of the kits as the error rate of false-positive results. Moreover, this study aims to minimize the total network cost and decrease false results through specificity and sensitivity characteristics. The fuzzy approach (PCCP model) is used to cope with the EU of input data, based on $\mathcal{M}e$ measure. Finally, the FMOGP was employed to solve the multi-objective model.

This paper investigates the issues raised during the C-19 outbreak and considers a real case of Iran to deal with risks, such as errors in the testing result (i.e., false results). In addition, a set of sensitivity analyses are performed. Our proposed C-19TKSN is applicable for an epidemic situation like the C-19 epidemic. It suggests the governments simultaneously coordinate location, distribution, and demand of C-19 test kits fulfillment decisions.

The application of the C-19TKSN results in the following managerial insights:

1. The nature of the C-19TKSN problem is dynamic over time due to difficult predictions and changes in the number of C-19 patients. The potential demands relating to different regions of the suspected C-19 cases for various C-19 test kits are stochastic. Besides, the rate of prevalence of C-19 is uncertain and quite challenging to be predicted. To do this, the DMs of the C-19TKSN can benefit from using the MSSP model.
2. Using the gamma formula introduced in Section 3.1 and the error of the kits, DMs can adjust the best strategy for allocating kits to suspect C-19 cases with the lowest cost and least false test results.
3. Considering the MTLs for C-19 testing centers is useful from several points of view:
   - This feature causes suitable dispersion for C-19 testing centers. Thus, it reduces referrals and congestion in test centers, which causes a decrease in the rate of C-19 prevalence.
   - The purpose of establishing a MTLs is to reduce the prevalence of C-19 and the risk of false results; all 5 MTLs have been established in the MSSP model and

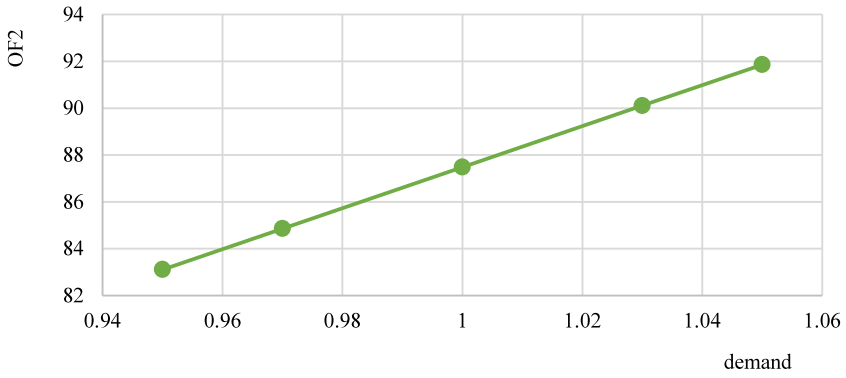

Fig. 17. The effect of changes in the potential demands of suspected C-19 cases' regions on the second OF.

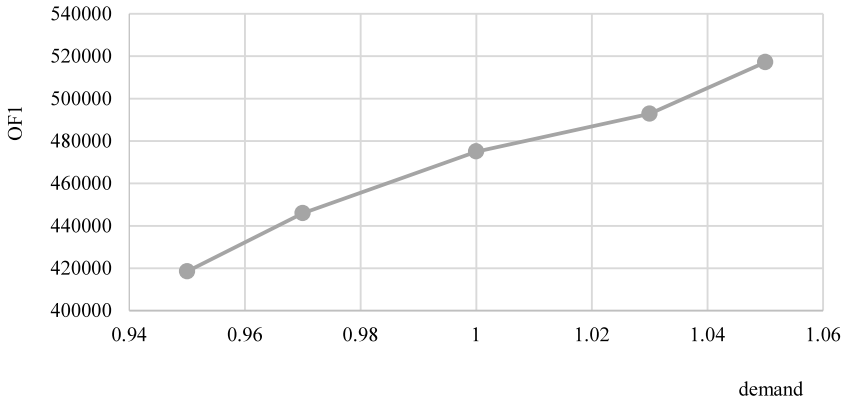

Fig. 18. The effect of changes in the potential demands of suspected C-19 cases' regions on the first OF.

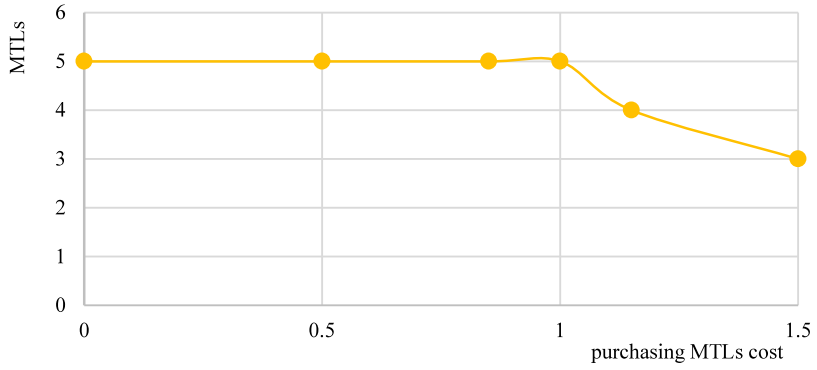

Fig. 19. The required number of MTLs by changing the purchasing MTLs cost.

have reduced the risk function of false results. In the MSSP model, updating each stage reduces costs like transportation, and thus the cost objective gets less value compared to the TSSP model.

- This feature performs the opened centers to disperse all over the region for covering more suspected C-19 cases. It leads to taking the C-19 test from different regions of suspected C-19 cases.
- Governments are able to manage the supply chain better by being informed of the potential services that would be necessary to serve the related centers.

6.1. Limitations and future studies

In this paper, we used gamma distribution based on the time between the emergence of their first symptoms and the time they are tested, so various C-19 test kits are allocated to the suspected C-19 cases with the best result and the lowest cost. This study is subject to several limitations. The suggested model can use various C-19 distributions in future studies such as:

- using gamma distribution based on the time between their first contact and the time they are tested
- using lognormal distribution based on the time between their first contact and the time they are hospitalized
- using lognormal distribution based on the time between the emergence of their first symptoms and the time they are hospitalized
- using lognormal distribution based on the time between their first contact and the time they are isolated
- using lognormal distribution based on the time between the emergence of their first symptoms and the time they are isolated

We suggest other research ways like using the weighted distance between the regions of suspected C-19 cases and testing centers and considering response time for C-19 test results.

CRediT authorship contribution statement

Seyyed-Mahdi Hosseini-Motlagh: Conceptualization, Formal analysis, Supervision. **Mohammad Reza Ghatreh Samani:** Conceptualization, Writing – review & editing, Methodology, Software. **Parnian Farokhnejad:** Investigation, Writing – original draft, Data curation, Software.

Declaration of competing interest

The authors declare that they have no known competing financial interests or personal relationships that could have appeared to influence the work reported in this paper.

Appendix A

The compact forms of the TSSP model for designing a C-19TKSN IS formulated as follows:

$$\mathcal{M}in\mathbb{E}[\mathcal{Z}] = \sum_{t} \mathcal{C}'.\mathcal{Y}_t + \pi_{\mathfrak{s}} \sum_{\mathfrak{s}} \mathcal{B}.\mathcal{X}_{t\mathfrak{s}}$$

Subject to

$$\sum_{\mathfrak{s}} \mathcal{X}_{t\mathfrak{s}} \le \mathcal{W}.\mathcal{Y}_t \quad \forall t$$

$$\mathcal{L}.\mathcal{X}_{t\mathfrak{s}} \ge d_{t\mathfrak{s}} \quad \forall \mathfrak{s}, t$$

$$\mathcal{V}.\mathcal{X}_{t\mathfrak{s}} = 0 \quad \forall \mathfrak{s}, t$$

$$\mathcal{H}.\mathcal{Y}_t \le 1 \quad \forall t$$

$$\mathcal{X}_{t\mathfrak{s}} \le \mathcal{M}.\mathcal{P}_{t\mathfrak{s}} \quad \forall \mathfrak{s}, t$$

$$\mathcal{P}_{t\mathfrak{s}} = \mathcal{P}_{t\mathfrak{s}'} \quad \forall t \in T(\mathfrak{s}, \mathfrak{s}') \in \mathcal{S}$$

$$\mathcal{P}_{t\mathfrak{s}}, \mathcal{Y}_t \in \{0, 1\}, \mathcal{X}_{t\mathfrak{s}} \ge 0, \tag{A.1}$$

Appendix B

Structural properties of the proposed model

Model of section 3.5

In this paper, a mixed-integer linear programming model is developed to design C-19TKSN. The proposed network comprises of the regions of suspected C-19 cases, kit manufacturers' centers, FTLs, MTLs, and specialized hospitals. The first OF, Eq. (7) wants to minimize the costs of the network consists of purchasing cost of MTLs ($\sum_j \left(\mathcal{C}\mathcal{F}_j * \mathcal{N}\right)$), moving costs of each MTL ($\sum_{j'j''t}(\mathcal{X}_{j'j''t} * \mathcal{C}_{j'j''})$), the different kits transportation costs from manufacturers to MTLs ($\sum_{pjkt\mathfrak{s}} \mathcal{P}_{\mathfrak{s}} * \mathcal{Y}'^{\mathfrak{s}}_{pjkt} * \mathcal{T}rc'_{pj}$+), FTLs ($\sum_{plkt\mathfrak{s}} \mathcal{P}_{\mathfrak{s}} * \mathcal{Y}''^{\mathfrak{s}}_{plkt} * \mathcal{T}rc''_{pl}$) and specialized hospital ($\sum_{phkt\mathfrak{s}} \mathcal{P}_{\mathfrak{s}} * \mathcal{Y}'''^{\mathfrak{s}}_{phkt} * \mathcal{T}rc'''_{ph}$), PCR kits transportation costs from MTLs ($\sum_{jht\mathfrak{s}} \mathcal{P}_{\mathfrak{s}} * \mathcal{F}'^{\mathfrak{s}}_{jht} * \mathcal{FO}'_{jh}$) and, FTLs ($\sum_{lht\mathfrak{s}} \mathcal{P}_{\mathfrak{s}} * \mathcal{F}''^{\mathfrak{s}}_{lht} * \mathcal{FO}''_{lh}$) to hospitals, production costs of test kits which sent from manufacturers to MTLs ($\sum_{pjtk\mathfrak{s}} \mathcal{P}_{\mathfrak{s}} * \mathcal{P}\mathcal{C}_k * \mathcal{Y}'^{\mathfrak{s}}_{pjkt}$), FTLs ($\sum_{pltk\mathfrak{s}} \mathcal{P}_{\mathfrak{s}} * \mathcal{P}\mathcal{C}_k * \mathcal{Y}''^{\mathfrak{s}}_{plkt}$), and specialized hospital ($\sum_{phtk\mathfrak{s}} \mathcal{P}_{\mathfrak{s}} * \mathcal{P}\mathcal{C}_k * \mathcal{Y}'''^{\mathfrak{s}}_{phkt}$), and finally operating costs in MTLs ($(|T|) * \sum_j \mathcal{OC}_j$), FTLs ($(|T|) * \sum_l \mathcal{OC}'_l$), and specialized hospitals ($(|T|) * \sum_h \mathcal{OC}''_h$), according to the possibility of different scenarios.

The second OF, Eq. (8), minimizes the risk of testing false results by allocating proper test kits. To apply the fundamental characteristics of diagnostic tests for C-19 disease (i.e., sensitivity, specificity), we divide the suspected C-19 cases into two groups of infected and uninfected based on the prevalence rate. In the 1st($\sum_{mjkrt\mathfrak{s}} \mathcal{P}_{\mathfrak{s}} * ((1-\eta_{rk}) * \mathcal{P}^{\mathfrak{s}}_{mjkrt} * prev^{\mathfrak{s}}_{mt})$), 2nd($\sum_{mlkrt\mathfrak{s}} \mathcal{P}_{\mathfrak{s}} * ((1-\eta_{rk}) * \mathcal{P}'^{\mathfrak{s}}_{mlkrt} * prev^{\mathfrak{s}}_{mt})$), and 3rd ($\sum_{mhkrt\mathfrak{s}} \mathcal{P}_{\mathfrak{s}} * ((1-\eta_{rk}) * \mathcal{P}''^{\mathfrak{s}}_{mhkrt} * prev^{\mathfrak{s}}_{mt})$) terms, by considering the infected C-19 cases who are testing ($\mathcal{P}'^{\mathfrak{s}}_{mlkrt} * prev^{\mathfrak{s}}_{m}$) and also the sensitivity coefficient (η_{rk}), the false-negative results have been reduced. The sensitivity coefficient (η_{rk}) is calculated according to the gamma formula in Section 3.1. Also, in the 4th ($\sum_{mjkrt\mathfrak{s}} \mathcal{P}_{\mathfrak{s}} * (\mathcal{B}_k * \mathcal{P}^{\mathfrak{s}}_{mjkrt} * (1-prev^{\mathfrak{s}}_{mt}))$), 5th ($\sum_{mlkrt\mathfrak{s}} \mathcal{P}_{\mathfrak{s}} * (\mathcal{B}_k * \mathcal{P}'^{\mathfrak{s}}_{mlkrt} * (1-prev^{\mathfrak{s}}_{mt}))$), and 6th ($\sum_{mhkrt\mathfrak{s}} \mathcal{P}_{\mathfrak{s}} * (\mathcal{B}_k * \mathcal{P}''^{\mathfrak{s}}_{mhkrt} * (1-prev^{\mathfrak{s}}_{m}))$) terms, by considering the uninfected cases who test ($\mathcal{P}^{\mathfrak{s}}_{mjkrt} * (1-prev^{\mathfrak{s}}_{mt})$) and also the specificity coefficient ($\mathcal{B}_k$), the false-positive results have been reduced. Specificity coefficient ($(\mathcal{B}_k)$) is calculated according to the failure percentage of each kit.

We assume m regions in the selected area, and we also assume infected and uninfected C-19 diseases of each region as suspected C-19 cases. The model aims to determine the optimal number of suspected C-19 cases of each region and assign them to the MTLs, FTLs, and specialized hospitals efficiently. Also, assign of the kits to suspected C-19 cases is based on minimizing the risk of allocating kits and minimizing cost.

Besides the assumption, the demand of various C-19 test kits (i.e., the total of the suspected C-19 cases) should be satisfied, which is shown by constraint (9). In other words, this constraint indicates that the total number of suspected C-19 cases go to MTLs, FTLs, and specialized hospitals for performing various C-19 test kits is equal to the total number of the suspected C-19 cases. Thus, the total number of various C-19 kits sent to MTLs, FTLs, and specialized hospitals should be greater than the number of suspected C-19 cases tested in MTLs, FTLs, and specialized hospitals, which this fact is shown by constraints (10)–(12), respectively.

It is obvious that the suspected C-19 cases can be assigned to open FTLs, MTLs, or specialized hospitals, which are shown by constraints (13)–(15), respectively. All the selected regions of suspected C-19 cases on the rth day can refer to one FTL or MTL or specialized hospitals which is shown by constraint (16).

In this study, three methods are available for the C-19 test; each kit has a maximum production capacity. Therefore, the number of various kits cannot be more than the maximum production capacity, which is indicated by constraint (17).

As mentioned earlier, three methods are available for testing C-19, which are different in cost and efficiency. Due to the high cost of PCR testing equipment, the required equipment for the PCR test is only provided in specialized hospitals. For this reason, PCR kits that are used in MTLs and FTLs should be sent to specialized hospitals. Thus, constraints (18) and (19) ensure that the number of PCR kits tested in MTLs, FTLs is equal to the used PCR kits which sent to the specialized hospital. Also, the input flow to a center should be lower than the capacity of that center, which this fact is indicated by constraints (20)–(22) for MTLs, FTLs and, specialized hospitals. The number of various C-19 kits sent to MTLs, FTLs does not exceed the maximum capacity of FTLs and also the sum of the number of various C-19 kits sent to specialized hospitals and the number of PCR kits sent to the specialized hospital for testing from MTLs, FTLs does not exceed the maximum capacity of specialized hospitals.

In order to reduce referrals and reduce congestion in test centers, which can lead to a high prevalence of the C-19 disease, MTLs are provided in some areas to improve access for people and reduce the movement and transportation of people among areas and reduce the prevalence of the C-19 disease. Therefore, constraints (23) and (24) indicate that only one MTL can be transferred to another candidate region of C-19 suspected cases in each period. Relocation of a MTL is possible in two consecutive periods only if it was in the previous location in the previous period, which was indicated by constraint (25). The number of required MTLs In each period is expressed by constraints (26).

Table C.1
Characteristics of parameters for stochastic parameter generation.

Symbol		Value
d'_{mt}	$\forall m, t$	U[800,1200]
δ_m	$\forall m$	U[$\sqrt{2}$,$\sqrt{2}+0.5$]
$\sigma(\varepsilon_m^N)$	$\forall m$	U[0.13,0.18]
$prev_{mt}'$	$\forall m$,t	U[0.001,0.008]
δ_m'	$\forall m$	U[1, $1+\sqrt{2}$]
$\sigma(\varepsilon_m^N)$	$\forall m$	U[0.1,0.12]

Table C.2
The list of hospitals and laboratories names in Tehran's 10th district.

Number	The region of suspected C-19 cases	Specialized hospitals/ FTLs name
1	1	Azadi Hospital
2	1	Yadegar Clinic
3	1	Maymanat Hospital
4	2	Shahriar Hospital
5	2	Eghbal Hospital
6	2	Lolagar Hospital
7	3	Babak Hospital
8	7	Hekmat Clinic
9	10	Shahidfahmideh Hospital
10	16	Ziaeian Hospital
11	4	Jeyhoon Laboratory
12	6	Borhan Laboratory
13	5	Ghasr Laboratory
14	13	Bina Laboratory

Appendix C

See Tables C.1 and C.2.

References

[1] Pneumonia of Unknown Cause China: Disease Outbreak News, World Health Organization, Geneva, 2020, January 5, https://www.who.int/csr/don/05-january-2020-pneumonia-of-unkown-cause-china/en/.

[2] E. De Wit, N. Van Doremalen, D. Falzarano, V.J. Munster, SARS and MERS: recent insights into emerging coronaviruses, Nat. Rev. Microbiol. 14 (8) (2016) 523.

[3] A.S. Fauci, H.C. Lane, R.R. Redfield, Covid-19—navigating the uncharted, 2020, http://dx.doi.org/10.1056/NEJMe2002387.

[4] World Health Organization, Laboratory testing strategy recommendations for COVID-19, 2020, 22 Mar. https://apps.who.int/iris/bitstream/handle/10665/331509/WHO-COVID-19-lab_testing-2020.1-eng.pdf.

[5] C.P. West, V.M. Montori, P. Sampathkumar, COVID-19 testing: the threat of false-negative results, in: Mayo Clinic Proceedings, vol. 95, no. 6, Elsevier, 2020, pp. 1127–1129, June http://dx.doi.org/10.1016/j.mayocp.2020.04.004.

[6] J.M. Sharfstein, S.J. Becker, M.M. Mello, Diagnostic testing for the novel coronavirus, JAMA 323 (15) (2020) 1437–1438, http://dx.doi.org/10.1001/jama.2020.3864.

[7] D. Ivanov, Predicting the impacts of epidemic outbreaks on global supply chains: A simulation-based analysis on the coronavirus outbreak (COVID-19/SARS-CoV-2) case, Transp. Res. E 136 (2020) 101922, http://dx.doi.org/10.1016/j.tre.2020.101922.

[8] R. Li, S. Pei, B. Chen, Y. Song, T. Zhang, W. Yang, J. Shaman, Substantial undocumented infection facilitates the rapid dissemination of novel coronavirus (SARS-CoV-2), Science 368 (6490) (2020) 489–493, http://dx.doi.org/10.1126/science.abb3221.

[9] Y. Dong, X.I. Mo, Y. Hu, X. Qi, F. Jiang, Z. Jiang, S. Tong, Epidemiological characteristics of 2143 pediatric patients with 2019 coronavirus disease in China, Pediatrics 145 (6) (2020) e20200702, http://dx.doi.org/10.1542/peds.2020-0702.

[10] G. Laporte, S. Nickel, F. Saldanha-da Gama, Introduction to location science, in: Location Science, Springer, Cham, 2019, pp. 1–21, http://dx.doi.org/10.1007/978-3-030-32177-2_1.

[11] M. Mousazadeh, S.A. Torabi, M.S. Pishvaee, F. Abolhassani, Health service network design: a robust possibilistic approach, Int. Trans. Oper. Res. 25 (1) (2018) 337–373, http://dx.doi.org/10.1111/itor.12417.

[12] S.A. Torabi, J. Namdar, S.M. Hatefi, F. Jolai, An enhanced possibilistic programming approach for reliable closed-loop supply chain network design, Int. J. Prod. Res. 54 (5) (2016) 1358–1387, http://dx.doi.org/10.1080/00207543.2015.1070215.

[13] K. Govindan, H. Mina, B. Alavi, A decision support system for demand management in healthcare supply chains considering the epidemic outbreaks: A case study of coronavirus disease 2019 (COVID-19), Transp. Res. E 138 (2020) 101967, http://dx.doi.org/10.1016/j.tre.2020.101967.

[14] D. Ivanov, A. Dolgui, Viability of intertwined supply networks: extending the supply chain resilience angles towards survivability. A position paper motivated by COVID-19 outbreak, Int. J. Prod. Res. 58 (10) (2020) 2904–2915, http://dx.doi.org/10.1080/00207543.2020.1750727.

[15] H. Yu, X. Sun, W.D. Solvang, X. Zhao, Reverse logistics network design for effective management of medical waste in epidemic outbreaks: insights from the coronavirus disease 2019 (COVID-19) outbreak in Wuhan (China), Int. J. Environ. Res. Public Health 17 (5) (2020) 1770, http://dx.doi.org/10.3390/ijerph17051770.

[16] D. Ivanov, Viable supply chain model: integrating agility, resilience and sustainability perspectives—lessons from and thinking beyond the COVID-19 pandemic, Ann. Oper. Res. (2020) 1–21, http://dx.doi.org/10.1007/s10479-020-03640-6.

[17] T.M. Choi, Innovative "bring-service-near-your-home" operations under corona-virus (COVID-19/SARS-CoV-2) outbreak: Can logistics become the messiah? Transp. Res. E 140 (2020) 101961, http://dx.doi.org/10.1016/j.tre.2020.101961.

[18] S. Kargar, M. Pourmehdi, M.M. Paydar, Reverse logistics network design for medical waste management in the epidemic outbreak of the novel coronavirus (COVID-19), Sci. Total Environ. 746 (2020) 141183, http://dx.doi.org/10.1016/j.scitotenv.2020.141183.

[19] S.K. Paul, P. Chowdhury, A production recovery plan in manufacturing supply chains for a high-demand item during COVID-19, Int. J. Phys. Distrib. Logist. Manage. (2020) http://dx.doi.org/10.1108/IJPDLM-04-2020-0127.

[20] C.L. Karmaker, T. Ahmed, S. Ahmed, S.M. Ali, M.A. Moktadir, G. Kabir, Improving supply chain sustainability in the context of COVID-19 pandemic in an emerging economy: Exploring drivers using an integrated model, Sustain. Prod. Consum. 26 (2021) 411–427, http://dx.doi.org/10.1016/j.spc.2020.09.019.

[21] Y. Li, K. Chen, S. Collignon, D. Ivanov, Ripple effect in the supply chain network: Forward and backward disruption propagation, network health and firm vulnerability, European J. Oper. Res. 291 (3) (2021) 1117–1131, http://dx.doi.org/10.1016/j.ejor.2020.09.053.

[22] M. Mousazadeh, S.A. Torabi, M.S. Pishvaee, F. Abolhassani, Accessible, stable, and equitable health service network redesign: A robust mixed possibilistic-flexible approach, Transp. Res. E 111 (2018) 113–129, http://dx.doi.org/10.1016/j.tre.2018.01.006.

[23] A. Lucchese, A. Marino, L. Ranieri, Minimization of the logistic costs in healthcare supply chain: a hybrid model, Procedia Manuf. 42 (2020) 76–83, http://dx.doi.org/10.1016/j.promfg.2020.02.025.

[24] S. Beheshtifar, A. Alimoahmmadi, A multiobjective optimization approach for location–allocation of clinics, Int. Trans. Oper. Res. 22 (2) (2015) 313–328, http://dx.doi.org/10.1111/itor.12088.

[25] D. Shishebori, A.Y. Babadi, Robust and reliable medical services network design under uncertain environment and system disruptions, Transp. Res. E 77 (2015) 268–288, http://dx.doi.org/10.1016/j.tre.2015.02.014.

[26] N. Zarrinpoor, M.S. Fallahnezhad, M.S. Pishvaee, Design of a reliable hierarchical location–allocation model under disruptions for health service networks: A two-stage robust approach, Comput. Ind. Eng. 109 (2017) 130–150, http://dx.doi.org/10.1016/j.cie.2017.04.036.

[27] A. Mohamadi, S. Yaghoubi, A bi-objective stochastic model for emergency medical services network design with backup services for disasters under disruptions: an earthquake case study, Int. J. Disaster Risk Reduct. 23 (2017) 204–217, http://dx.doi.org/10.1016/j.ijdrr.2017.05.003.

[28] P. Wikramaratna, R.S. Paton, M. Ghafari, J. Lourenco, Estimating false-negative detection rate of SARS-CoV-2 by RT-PCR, MedRxiv (2020) http://dx.doi.org/10.1101/2020.04.05.20053355.

[29] B. Zahiri, S.A. Torabi, M. Mohammadi, M. Aghabegloo, A multi-stage stochastic programming approach for blood supply chain planning, Comput. Ind. Eng. 122 (2018) 1–14, http://dx.doi.org/10.1016/j.cie.2018.05.041.

[30] J.R. Birge, F. Louveaux, Introduction to Stochastic Programming, Springer Science & Business Media, 2011.

[31] M. Fattahi, K. Govindan, E. Keyvanshokooh, Responsive and resilient supply chain network design under operational and disruption risks with delivery lead-time sensitive customers, Transp. Res. E 101 (2017) 176–200, http://dx.doi.org/10.1016/j.tre.2017.02.004.

[32] B. Zahiri, S.A. Torabi, R. Tavakkoli-Moghaddam, A novel multi-stage possibilistic stochastic programming approach (with an application in relief distribution planning), Inform. Sci. 385 (2017) 225–249, http://dx.doi.org/10.1016/j.ins.2017.01.018.

[33] E. Surkova, V. Nikolayevskyy, F. Drobniewski, False-positive COVID-19 results: hidden problems and costs, Lancet Respir. Med. 8 (12) (2020) 1167–1168, http://dx.doi.org/10.1016/S2213-2600(20)30453-7.
[34] I. Arevalo-Rodriguez, D. Buitrago-Garcia, D. Simancas-Racines, P. Zambrano-Achig, R. Del Campo, A. Ciapponi, O. Sued, L. Martinez-Garcia, A.W. Rutjes, N. Low, P.M. Bossuyt, False-negative results of initial RT-PCR assays for COVID-19: a systematic review, PLoS One 15 (12) (2020) e0242958.
[35] D. Willman, Contamination At CDC Lab Delayed Rollout of Coronavirus Tests, Washington Post, 2020.
[36] J. Dupačová, N. Gröwe-Kuska, W. Römisch, Scenario reduction in stochastic programming, Math. Program. 95 (3) (2003) 493–511, http://dx.doi.org/10.1007/s10107-002-0331-0.
[37] M.S. Sodhi, Managing demand risk in tactical supply chain planning for a global consumer electronics company, Prod. Oper. Manage. 14 (1) (2005) 69–79, http://dx.doi.org/10.1111/j.1937-5956.2005.tb00010.x.
[38] J. Dupačová, Multistage stochastic programs: The state-of-the-art and selected bibliography, Kybernetika 31 (2) (1995) 151–174.
[39] H. Heitsch, W. Römisch, Scenario reduction algorithms in stochastic programming, Comput. Optim. Appl. 24 (2) (2003) 187–206, http://dx.doi.org/10.1023/A:1021805924152.
[40] H. Heitsch, W. Romisch, Generation of multivariate scenario trees to model stochasticity in power management, in: 2005 IEEE Russia Power Tech, IEEE, 2005, pp. 1–7, June, http://dx.doi.org/10.1109/PTC.2005.4524696.
[41] N. Growe-Kuska, H. Heitsch, W. Romisch, Scenario reduction and scenario tree construction for power management problems, in: 2003 IEEE Bologna Power Tech Conference Proceedings, vol. 3, IEEE, 2003, p. 7, June, http://dx.doi.org/10.1109/PTC.2003.1304379.
[42] M.R.G. Samani, S.M. Hosseini-Motlagh, An enhanced procedure for managing blood supply chain under disruptions and uncertainties, Ann. Oper. Res. 283 (1) (2019) 1413–1462, http://dx.doi.org/10.1007/s10479-018-2873-4.
[43] M. Inuiguchi, J. Ramık, Possibilistic linear programming: a brief review of fuzzy mathematical programming and a comparison with stochastic programming in portfolio selection problem, Fuzzy Sets and Systems 111 (1) (2000) 3–28, http://dx.doi.org/10.1016/S0165-0114(98)00449-7.
[44] B. Liu, K. Iwamura, Chance constrained programming with fuzzy parameters, Fuzzy Sets and Systems 94 (2) (1998) 227–237, http://dx.doi.org/10.1016/S0165-0114(96)00236-9.
[45] B. Liu, Y.K. Liu, Expected value of fuzzy variable and fuzzy expected value models, IEEE Trans. Fuzzy Syst. 10 (4) (2002) 445–450, http://dx.doi.org/10.1109/TFUZZ.2002.800692.
[46] J. Xu, X. Zhou, Approximation based fuzzy multi-objective models with expected objectives and chance constraints: Application to earth-rock work allocation, Inform. Sci. 238 (2013) 75–95, http://dx.doi.org/10.1016/j.ins.2013.02.011.
[47] H.J. Zimmermann, Fuzzy programming and linear programming with several objective functions, Fuzzy Sets and Systems 1 (1) (1978) 45–55, http://dx.doi.org/10.1016/0165-0114(78)90031-3Get.
[48] M. Sakawa, H. Yano, An interactive satisficing method for multiobjective nonlinear programming problems with fuzzy parameters, in: Optimization Models using Fuzzy Sets and Possibility Theory, Springer, Dordrecht, 1987, pp. 258–271, http://dx.doi.org/10.1007/978-94-009-3869-4_18.
[49] T. Kundu, S. Islam, An interactive weighted fuzzy goal programming technique to solve multi-objective reliability optimization problem, J. Ind. Eng. Int. 15 (1) (2019) 95–104, http://dx.doi.org/10.1007/s40092-019-0321-y.
[50] C.F. Hu, C.J. Teng, S.Y. Li, A fuzzy goal programming approach to multi-objective optimization problem with priorities, European J. Oper. Res. 176 (3) (2007) 1319–1333, http://dx.doi.org/10.1016/j.ejor.2005.10.049.
[51] S.M. Hosseini-Motlagh, M.R.G. Samani, V. Shahbazbegian, Innovative strategy to design a mixed resilient-sustainable electricity supply chain network under uncertainty, Appl. Energy 280 (2020) 115921, http://dx.doi.org/10.1016/j.apenergy.2020.115921.
[52] K. Huang, S. Ahmed, The value of multistage stochastic programming in capacity planning under uncertainty, Oper. Res. 57 (4) (2009) 893–904, http://dx.doi.org/10.1287/opre.1080.0623.
[53] Z. Hu, G. Hu, A multi-stage stochastic programming for lot-sizing and scheduling under demand uncertainty, Comput. Ind. Eng. 119 (2018) 157–166, http://dx.doi.org/10.1016/j.cie.2018.03.033.